## Standard platinum resistance thermometer interpolations in a revised temperature scale

White, D. R.; Rourke, P. M. C.



**Publisher's version / Version de l'éditeur:**
https://doi.org/10.1088/1681-7575/ab6b3c
*Metrologia, 57, 3, 2020-05-26*

Metrologia



# Standard platinum resistance thermometer interpolations in a revised temperature scale

To cite this article before publication: D Rod White *et al* 2020 *Metrologia* in press https://doi.org/10.1088/1681-7575/ab6b3c

# STANDARD PLATINUM RESISTANCE THERMOMETER INTERPOLATIONS IN A REVISED TEMPERATURE SCALE

D R White
Measurement Standards Laboratory
PO Box 31310 Lower Hutt, New Zealand
rod.white@measurement.govt.nz

P M C Rourke
National Research Council
1200 Montreal Rd., Ottawa, Ontario, Canada
Patrick.Rourke@nrc-cnrc.gc.ca

## ABSTRACT

The thermal metrology community is considering revising the International Temperature Scale of 1990 (ITS-90), motivated by the opportunity to improve the thermodynamic accuracy, reproducibility, and ease of use of the scale, as well as health and safety concerns with the use of mercury in the current scale. This paper considers the mathematical structure of the Standard Platinum Resistance Thermometer (SPRT) interpolations of the ITS-90 and identifies (i) mathematical features that are advantageous and should be retained, (ii) opportunities for improvements, and (iii) the research required to maximise the benefits from such improvements. The improvements considered include minor adjustments that leave ITS-90 intact, numerical adjustments to reference resistance ratios that preserve the structure of ITS-90, fixed-point replacements, new subranges, and large-scale changes in the mathematical structure of the interpolations. A significant research effort will be required to implement some of the changes. Overall, an improvement in the thermodynamic accuracy by a factor of about 10 is relatively easily realised, but improvements in reproducibility of the scale of even a couple of tens of percent will be hard won. For most users, the costs and inconvenience of a substantial scale revision may outweigh the benefits.

## 1. INTRODUCTION

The International Temperature Scale of 1990 (ITS-90) has been in use for 30 years, longer than any previous international temperature scale (ITS) [1, 2]. While it has been very successful and is now tightly integrated into the world's measurement infrastructure, it has known shortcomings [3, 4]. Now that the SI revision is complete [5, 6], many research groups are turning from Boltzmann constant determinations to measurements of the differences between thermodynamic temperatures and ITS-90 temperatures, with a view to improving the ITS.

Historically, the ITS has been revised every 20 years or so, with each revision offering a greater thermodynamic accuracy and better reproducibility and covering a wider temperature range than its precursor. One consequence of the recent drive for low-uncertainty determinations of the Boltzmann constant is that there have been substantial improvements in primary thermometry, and there are now three primary techniques, acoustic gas thermometry [7-11], dielectric constant gas thermometry [12, 13], and Johnson noise thermometry [14, 15], capable of measuring thermodynamic temperatures near 300 K with uncertainties of 1 mK or less. Indeed, it is now possible to make thermodynamic measurements with uncertainties below the irreproducibility of the ITS-90 [16]. However, it does not immediately follow that ITS-90 is obsolete, or that an ITS is unnecessary [17]. Except perhaps for temperatures below 1 K and above 1300 K, thermodynamic temperature measurements remain impracticably difficult, time consuming, and costly compared to realisation of an ITS, so an ITS will be required for some time. The new techniques do, however, offer the possibly of a new ITS that is a substantially better approximation of the thermodynamic temperature scale.

Perhaps the most compelling reason to consider a new ITS is the increasing recognition of health and safety hazards. Mercury, an essential component of the ITS-90 for temperatures below 0 °C, is toxic and, in some countries, health and safety legislation is making it increasingly difficult to operate a mercury-triple-point apparatus. Such difficulties will increase as the United Nations Environmental Programme's (UNEP) Minamata Convention on Mercury [18] takes force over the next decade or so. The convention, which has been ratified by over 100 countries, plans for the gradual world-wide elimination of the mining, trade, and use of mercury.

Mercury is also an air-transport hazard. Liquid mercury dissolves aluminium forming a liquid amalgam allowing the aluminium to react with air and oxidise. In this way, mercury catalyses the rapid oxidation of aluminium. Most airlines refuse to ship mercury because of the potential for major structural damage, even with small spills. Gallium, a less important but still useful ITS-90 fixed point, is also an air-transport hazard, and many airlines require it to be packed with refrigerants such as dry ice. However, unlike the case for mercury, it is unlikely that gallium regulations will become more restrictive in the future, and the shipment of gallium by sea exists as an alternative option.

Another factor favouring a new ITS is a better understanding of the origin of irreproducibility (non-uniqueness) in interpolated scales [19]. For the most part, ITS-90 was founded on numerical experiments with resistance-temperature data from a selection of SPRTs. Many of these experiments are recorded in the working documents of the CIPM Consultative Committee for Thermometry (CCT) for 1984, 1987 and 1989 [20-22]. While there have been several efforts to establish a theoretical basis for interpolating equations [23-30], none have been satisfactory. Consequently, the ITS-90 interpolating equations are mathematical approximations rather than physical models. Now, with a better understanding of the application of approximation theory to calibration equations and the causes and effects of interpolation error [31-33], there is a possibility of developing a new ITS with improved reproducibility.

This paper focuses on the work that might be required to revise the Standard Platinum Resistance Thermometer (SPRT) subranges of the ITS-90. These are the parts of ITS-90 least likely to be replaced by thermodynamic techniques anytime soon. Section 2 first summarizes what we know of the structure and properties of ITS-90 with a focus on the consequences and utility of those properties. The section also resolves some common misunderstandings and includes new observations about the nature of non-uniqueness. Section 3 builds on Section 2 to identify options for future scale development. These options are evaluated in terms of potential advantages, disadvantages, and the work required to support them. Finally, Section 4 summarises the conclusions and briefly comments on the costs and benefits of a new scale.

## 2. STRUCTURE AND PROPERTIES OF ITS-90

### 2.1 The Interpolations

The SPRT subranges of the ITS-90 define temperature in terms of the electrical resistance of SPRTs, employing three distinct mathematical steps. Firstly, a measured SPRT resistance at any temperature, $R(T)$, is normalized with respect to the resistance at the triple point of water (TPW), $R_{\mathrm{H2O}} = R(0.01\ ^\circ\mathrm{C}) = R(273.16\ \mathrm{K})$, by calculating the resistance ratio:

$$W = W(T) = \frac{R(T)}{R_{\mathrm{H2O}}}. \tag{1}$$

Secondly, each SPRT is used to interpolate between the reference resistance ratios, $W_{\mathrm{r},i}$, defined for each fixed point, using an equation passing through the points (1, 1), ($W_2$, $W_{\mathrm{r}2}$), …, ($W_N$, $W_{\mathrm{r}N}$), where $W_i$ are the measured resistance ratios for each fixed point. The interpolations are all defined by ITS-90 in the form

$$W - W_{\mathrm{r}}(W) = \Delta W(W), \tag{2}$$

where $W_{\mathrm{r}}(W)$ is the reference resistance ratio and the deviation functions, $\Delta W(W)$, are specified polynomials in $W$– 1 and/or ln($W$). Finally, the temperature is calculated using $T_{90}(W_{\mathrm{r}})$, the inverse of the defined $W_{\mathrm{r}}(T_{90})$ reference function. The function $W_{\mathrm{r}}(T_{90})$ is exact, one-to-one, and defined in two segments: one for temperatures below 0.01 °C, and one for temperatures above 0 °C.

All the ITS-90 SPRT interpolation equations are linear with respect to their coefficients, so can be rewritten in the form [19, 34, 35]

$$W_{\mathrm{r}}(W) = \sum_{i=1}^{N} W_{\mathrm{r},i} F_i(W), \tag{3}$$

where the reference resistance ratios, $W_{r,i}$, are now the coefficients in the interpolating equation and the interpolating functions, $F_i(W)$, are functions of measured resistance ratios only. In (3), and the discussion that follows, the fixed-point resistance ratios and interpolating functions are enumerated by the subscripted index $i$, which may be numeric or the chemical symbol for the corresponding fixed-point substance. Leading superscripts on the functions may be used to distinguish the subrange. For example, ${}^{\mathrm{Zn}}F_{\mathrm{Sn}}(W)$ is the interpolating function associated with the tin point in the water-zinc subrange. In all cases, a subscript of $i = 1$ corresponds to the triple point of water, for which the measured and reference resistance ratios are unity, by definition.

As will be shown shortly, knowledge of the interpolating functions, $F_i(W)$, is important because they are the sensitivity coefficients for uncertainty propagation and major factors influencing the reproducibility of the scale. The interpolating functions can be determined by first rewriting (2) to identify all the terms in the interpolating equation:

$$W_{\mathrm{r}}(W) = W - a\Delta W_2(W) - b\Delta W_3(W) - \ldots \ . \tag{4}$$

where $a$, $b$, …, are the usual ITS-90 coefficients determined from measurements of resistance ratio at the fixed points, $W_i$, and $\Delta W_i$ , with $i = 2..\ N$ are the terms in the deviation function. The full set of interpolating functions, $F_i(W)$, is then given by [19] (note that the signs of the coefficients in (4) can be ignored):

$$\begin{pmatrix} F_1(W) \\ F_2(W) \\ \vdots \\ F_N(W) \end{pmatrix} = \begin{pmatrix} 1 & W_2 & \cdots & W_N \\ \Delta W_2(1) & \Delta W_2(W_2) & \cdots & \Delta W_2(W_N) \\ \vdots & \vdots & \ddots & \vdots \\ \Delta W_N(1) & \Delta W_N(W_2) & \ldots & \Delta W_N(W_N) \end{pmatrix}^{-1} \begin{pmatrix} W \\ \Delta W_2(W) \\ \vdots \\ \Delta W_N(W) \end{pmatrix}, \tag{5}$$

where the identity $W_1 = W_{\mathrm{H2O}} = 1$ has been used. For example, the ITS-90 interpolating equation for the water-zinc subrange is rewritten as $W_{\mathrm{r}}(W) = W - a(W-1) - b(W-1)^2$ , so the interpolating functions are given by

$$\begin{pmatrix} F_{\mathrm{H2O}}(W) \\ F_{\mathrm{Sn}}(W) \\ F_{\mathrm{Zn}}(W) \end{pmatrix} = \begin{pmatrix} 1 & W_{\mathrm{Sn}} & W_{\mathrm{Zn}} \\ 0 & W_{\mathrm{Sn}} - 1 & W_{\mathrm{Zn}} - 1 \\ 0 & (W_{\mathrm{Sn}} - 1)^2 & (W_{\mathrm{Zn}} - 1)^2 \end{pmatrix}^{-1} \begin{pmatrix} W \\ W - 1 \\ (W-1)^2 \end{pmatrix}. \tag{6}$$

Algebraic expressions for the interpolating functions for most of the ITS-90 SPRT interpolations are given in [35]. Approximate expressions for the $F_{\mathrm{i}}(W)$, sufficiently accurate for uncertainty analysis (but not interpolation), can be obtained by using the $W_{\mathrm{r,i}}$ values in place of the $W_{\mathrm{i}}$ values in (6).

During the development of ITS-90, the interpolating functions were determined numerically and used to compute the sensitivity of scale temperature to fixed-point errors [3, 4]. However, the sensitivity coefficients given for triple-point-of-water measurements were incorrect, a point first noted by Bloembergen [36].

The interpolating functions fall into two groups: Lagrange polynomials, and the remainder. All the interpolating functions for the subranges between the mercury and aluminium points are Lagrange polynomials, so have the form [31-33]:

$$F_i(W) = \prod_{\substack{m=1 \\ m \neq i}}^{N} \left( \frac{W - W_m}{W_i - W_m} \right). \tag{7}$$

For example, the interpolating function corresponding to the tin point in the water-aluminium subrange is the third-order Lagrange polynomial

$${}^{\mathrm{Al}}F_{\mathrm{Sn}}(W) = \frac{(W-1)(W-W_{\mathrm{Zn}})(W-W_{\mathrm{Al}})}{(W_{\mathrm{Sn}}-1)(W_{\mathrm{Sn}}-W_{\mathrm{Zn}})(W_{\mathrm{Sn}}-W_{\mathrm{Al}})}. \tag{8}$$

Figure 1 plots the four interpolating functions for the water-aluminium subrange. In some places the interpolating functions have magnitudes greater than 1.0, which means they amplify measurement uncertainties and non-uniqueness (see Secs. 2.2 and 2.5 below).

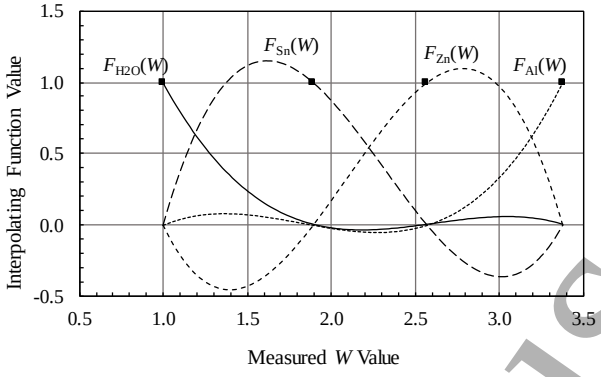


**Figure 1:** The four interpolating functions for the water–aluminium subrange of ITS-90.

For the aluminium-silver subrange and all subranges below 0.01 °C, the interpolating functions are not Lagrange polynomials, but they do possess some of the properties of Lagrange polynomials. All the interpolating functions have a type of orthonormality property: they take the value 1.0 at the fixed point for which they are named and are zero at all other fixed points (see Figure 1 for examples); that is,

$$F_i(W_j) = \begin{cases} 1, & j = i \\ 0, & j \neq i. \end{cases} \tag{9}$$

This property shows the functions $F_i(W)$ are linearly independent, as are the ITS-90-defined functions on the right-hand side of (4), and both sets of functions are basis functions for the same $N$-dimensional vector space. Any function $g(W)$ that lies within the vector space can be interpolated exactly and satisfies the following identity [19, 31, 34]

$$\sum_{i=1}^{N} g(W_i) F_i(W) = g(W). \tag{10}$$

That is, $g(W)$ can be determined completely from the $N$ measurements, $g(W_i)$, at the fixed points. Two of the identities suggested by (10), $\sum F_i(W) = 1$ and $\sum W_i F_i(W) = W$, apply to all of the ITS-90 SPRT subranges and are useful for simplifying algebraic expressions.

## 2.2 Propagation of Uncertainty

One of the advantages of writing the interpolations in the form of (3) is that the propagation-of-error equation can be written down directly in terms of the measured quantities; i.e., it avoids the complications of propagating errors through the ITS-90 coefficients, *a*, *b*, *c*, … [19]. The propagation-of-error equation is obtained by differentiating (3) with respect to the $2N+1$ variables in the equation

$$dW_r = \sum_{i=1}^{N} F_i(W) dW_{r,i} - \sum_{i=1}^{N} \left( \left. \frac{\partial W_r}{\partial W} \right|_{W=W_i} \right) F_i(W) dW_i + \left( \frac{\partial W_r}{\partial W} \right) dW, \tag{11}$$

where $W$ is the resistance ratio measured when the SPRT is used to determine an unknown temperature.

Where SPRTs are calibrated against fixed points, (11) can be simplified, as follows. Firstly, because the $W_{r,i}$ values are defined by ITS-90, the error terms $dW_{r,i}$ are zero. Secondly, the derivative $\partial W_r / \partial W$ is almost exactly equal to 1 (within 0.04% for all ITS-90 qualified SPRTs), and hence,

$$dW_r \approx -\sum_{i=2}^{N} F_i(W) dW_i + dW \,. \tag{12}$$

The summation in (12) excludes a term for the triple point of water ($i$ = 1), because $W_{H2O} = 1$ by definition.

Further computation using (12) is complicated by the common factor of $R_{H2O}$ in the $W_i$ values and correlations due to shared errors in triple-point-of-water measurements. This problem is overcome by expressing the $W_i$ values in terms of $R_{H2O}$ and the SPRT resistances at the various fixed-points, $R_i$:

$$dW_i = \frac{1}{R_{H2O}} \left[ dR_i - W_i dR_{H2O} \right]. \tag{13}$$

From this point, there are several possible cases to consider [35]. In the simplest case, which will suffice for the discussion here, a single value of the triple-point-of-water resistance is used to calculate all $W_i$ values, and the propagation-of-error equation, (12), simplifies to

$$dW_r = \frac{1}{R_{H2O}} \left( dR - \sum_{i=1}^{N} F_i(W) dR_i \right), \tag{14}$$

where $R$ is the SPRT resistance at the unknown temperature. Equation (14) now collects, under the summation, the propagated error of all the calibration measurements. Each interpolating function, $F_i(W)$, is a sensitivity coefficient describing the error propagation for a fixed point.

The equations for uncertainty propagation in the interpolated $W_r$ follow from (14). When all the contributing measurement uncertainties are uncorrelated:

$$u^2(W_r) = \left( \frac{1}{R_{H2O}} \right)^2 \left( u^2(R) + \sum_{i=1}^{N} F_i^2(W) u^2(R_i) \right), \tag{15}$$

and this is the simplest uncertainty propagation equation applicable to all ITS-90 interpolations. Note that the uncertainties associated with the SPRT calibrations, $u(R_i)$, are collated under the summation, while the uncertainty associated with the use of the SPRT (after calibration) is represented by the uncertainty $u(R)$. Where different triple-point-of-water measurements are used to normalise different resistance measurements, the equations are more complicated than (15) [35].

Equation (15) suggests two conclusions that may seem counterintuitive. Firstly, the right hand side of (15) is independent of the $W_r(T_{90})$ function, including the values of $W_{r,i}$ assigned to the fixed points. While there is a weak connection between $W_r$ and $W$ due to the assumption that $\partial W_r / \partial W \approx 1$, the uncertainties propagated from all resistance measurements are independent of the $W_r(T_{90})$ function and depend only on the interpolating equations and the measured $W_i$ values. That is, the scale uncertainty is independent of the $W_r(T_{90})$ definition. Secondly, the summation in (15) shows that the triple point of water does not have an elevated status amongst the fixed points; it is included in (15) in the same way as the other fixed points (see also Sec. 2.4).

## 2.3 Equivalent Interpolations – Part I

For those unfamiliar with the equations, it can be difficult to accept that the interpolations in terms of deviations, (2), and the interpolation direct to $W_r$, (3), are equivalent. In fact, by combining the direct interpolating equation, (3), with (10) for functions that are interpolated exactly, an infinite number of mathematically equivalent interpolations can be constructed:

$$W_{\mathrm{r}}(W) + g(W) = \sum_{i=1}^{N} \left[ W_{\mathrm{r},i} + g(W_i) \right] F_i(W) , \tag{16}$$

where $g(W)$ is any function that can be interpolated exactly. Such interpolations result in identical $W_{\mathrm{r}}$ values, identical interpolation error, and identical uncertainty propagation. All the ITS-90 interpolations interpolate the functions $g(W) = W$ and $g(W) = 1$ exactly, so amongst the equivalent interpolations are

$$W_{\mathrm{r}}(W) - W = \sum_{i=1}^{N} \left[ W_{\mathrm{r},i} - W_i \right] F_i(W) , \tag{17}$$

which is the ITS-90 formulation in terms of deviations (compare to (2)), and

$$W_{\mathrm{r}}(W) - 1 = \sum_{i=1}^{N} \left[ W_{\mathrm{r},i} - 1 \right] F_i(W) , \tag{18}$$

which is a helpful starting point when investigating subrange inconsistency (Sec. 2.6) [37]. But there are also an infinite number of equivalent interpolations with no obvious utility; for example, the equation

$$W_{\mathrm{r}}(W) - \ln(W) = \sum_{i=1}^{N} \left[ W_{\mathrm{r},i} - \ln(W_i) \right] F_i(W) , \tag{19}$$

is equivalent to the ITS-90 interpolation in the neon-water subrange, and the equation

$$W_{\mathrm{r}}(W) + 5W^3 = \sum_{i=1}^{N} \left[ W_{\mathrm{r},i} + 5W_i^3 \right] F_i(W) . \tag{20}$$

is equivalent to the ITS-90 interpolation for the water-aluminium subrange. Since $\ln(W)$ and $5W^3$ are among the functions that interpolate exactly, given appropriate basis functions $F_i(W)$, their inclusion on both sides of the above examples just needlessly increases the complexity of the equations without changing the interpolations in $W$.

One drawback of the ITS-90 formulation in terms of deviations is the illusion of an extra step in the mathematical process for calculating a temperature. As described in Sec. 2.1, the mathematical steps are $R \rightarrow W \rightarrow W_{\mathrm{r}} \rightarrow T_{90}$, while the ITS-90 definition of the interpolations has the appearance of $R \rightarrow W \rightarrow \Delta W \rightarrow W_{\mathrm{r}} \rightarrow T_{90}$, with the extra step potentially adding to confusion with mathematical analysis. The deviation-function formulation does have the advantage of resolving differences between SPRTs when plotting calibration data as deviations, and in times before computers, would have reduced the effects of round-off errors.

## 2.4 Equivalent Interpolations – Part II

It is instructive to multiply all the $W$ and $W_i$ variables in (8) by $R_{\mathrm{H_2O}}$, so that

$${}^{\mathrm{Al}}F_{\mathrm{Sn}}(W) = \frac{(W-1)(W-W_{\mathrm{Zn}})(W-W_{\mathrm{Al}})}{(W_{\mathrm{Sn}}-1)(W_{\mathrm{Sn}}-W_{\mathrm{Zn}})(W_{\mathrm{Sn}}-W_{\mathrm{Al}})} = \frac{(R-R_{\mathrm{H_2O}})(R-R_{\mathrm{Zn}})(R-R_{\mathrm{Al}})}{(R_{\mathrm{Sn}}-R_{\mathrm{H_2O}})(R_{\mathrm{Sn}}-R_{\mathrm{Zn}})(R_{\mathrm{Sn}}-R_{\mathrm{Al}})} . \tag{21}$$

When applied to all interpolating functions of a Lagrange interpolation, the interpolation is transformed to an interpolation in resistance rather than resistance ratio; i.e.

$$W_{\mathrm{r}}(R) = \sum_{i=1}^{N} W_{\mathrm{r},i} F_i(R) . \tag{22}$$

Note, too, in the right-hand side of (21) the measurement at the TPW appears in same way as the measurements at other fixed points.

Most of the ITS-90 interpolations possess a type of invariance property of which (21) is an example. If in any Lagrange interpolation the various $W$ variables are replaced by $Y = mW + c$, then the $m$ and $c$ parameters all cancel leaving the expressions for the interpolating functions unchanged. That is, for all values of $m$ (except $m = 0$) and $c$, the values of $W_r$ inferred using the equation are identical.

This invariance property means that the Lagrange interpolations of ITS-90 can be carried out not only in terms of $W$ and $R$, but also in terms of the resistance ratio indicated on a resistance bridge, the Cragoe variable [23]

$$Z(T) = \frac{R(T) - R_{\mathrm{H2O}}}{R(100\ ^{\circ}\mathrm{C}) - R_{\mathrm{H2O}}}, \tag{23}$$

and the residual-resistance ratio

$$RR(T) = \frac{R(T) - R(4\ \mathrm{K})}{R_{\mathrm{H2O}}}. \tag{24}$$

This observation clarifies some of the debate that preceded the development of the ITS-90 and earlier scales [20-23] regarding the effectiveness of interpolations using different variables: Lagrange interpolations in any of these variables are equivalent.

If an interpolation uses polynomials in the logarithm of the resistance ratio, e.g.,

$$W_r = A + B\ln(W) + C[\ln(W)]^2 + D[\ln(W)]^3, \tag{25}$$

then transformations of the form $Y = cW^m$ all yield the same interpolation.

Such scaling laws are desirable when thermometers are available with different resistance values, or perhaps some aspect of the sensor physics indicates that a particular scaling law might be applicable. Consider, as a counterexample, the Steinhart-Hart equation for thermistors [38]:

$$\frac{1}{T} = a_0 + a_1 \ln(R/R_0) + a_3\left[\ln(R/R_0)\right]^3, \tag{26}$$

where $R_0$ is the unit of resistance measurement, i.e., ohm, kilo-ohm, etc. The omission of the $\left[\ln(R/R_0)\right]^2$ term in (26), apparently because of numerical errors in the original analysis [39], causes inconsistent calibrations [40]. The problem can be seen by replacing $R_0$ by $\rho R_0$ in (26), where $\rho$ is a numerical constant:

$$\frac{1}{T} = a_0 + a_1\left[\ln\left(\frac{R}{R_0}\right) - \ln(\rho)\right] + a_3\left[\ln\left(\frac{R}{R_0}\right) - \ln(\rho)\right]^3, \tag{27}$$

so that a term in $\left[\ln(R/R_0)\right]^2$ emerges from the cubic term if $\rho$ is not equal to 1.0. Because the Steinhart-Hart equation cannot accommodate this term, it must yield different calibration equations with different interpolation errors and different uncertainty propagation whenever the units of measurement are changed (e.g., from ohms to kilo-ohms), when it's applied to thermistors of the same beta characteristic but different $R$(25 °C) values, or when nominally identical thermistors are connected in series or parallel .

The consistency of calibrations is an important consideration because SPRTs with widely different $R_{\mathrm{H2O}}$ values may be used for the same temperature range. There are two approaches for avoiding such inconsistencies. Firstly, the measured resistance can be normalized by a specific value of the sensor resistance, and this is the approach adopted by ITS-90 with the normalization by $R_{\mathrm{H2O}}$.

The second solution is to ensure the calibration equations form a complete sequence of nomials, as shown in (25). For most subranges of ITS-90, the sequences of functions are complete so that the substitution $Y = mW$ makes no difference to the interpolation. The two exceptions are the *e*-hydrogen-water and oxygen-water subranges, for

which the sequences of logarithms are not complete and the normalisation to $W$ is essential to eliminate calibration inconsistencies.

There are other practical reasons for retaining the calculation of the resistance ratio, $W$. Most significantly, the use of the resistance ratio eliminates the need to make resistance measurements traceable to the ohm, or equivalently, it eliminates uncertainties due to poorly calibrated resistance standards. With the formulation in terms of resistance ratio, it is sufficient that local resistance standards are stable over the duration of a set of measurements.

## 2.5 Interpolation Error/Non-uniqueness

For all functions lying outside the vector space spanned by the interpolating functions, the interpolation can only approximate the function's true behaviour and the interpolation is accompanied by interpolation error. Because the true resistance-temperature characteristic of every SPRT is influenced by numerous poorly understood physical effects, every SPRT response is slightly different and no SPRT interpolation is free of interpolation error. The different interpolation errors for different SPRTs and different interpolating equations give rise to variations in the interpolated values of $W_r$ between the fixed points. The variations are manifest as Type 3 non-uniqueness (NU3) if different SPRTs are compared, and Type 1 non-uniqueness (subrange inconsistency or SRI) if different equations are compared for the same SPRT [41, 42].

Figure 2 shows linear and quadratic interpolations of a $W_{r,ideal}(W)$ function with exaggerated non-linearity. The difference between the $W_{r,ideal}(W)$ curve and the interpolations is the interpolation error. If the $W_{r,ideal}(W)$ relations for different SPRTs have similar curvature, there will be consistent difference between all first- and second-order interpolations. Such a difference leads to a consistent bias between temperatures determined by the different equations, i.e., significant subrange inconsistency. This observation raises several important questions. Can we eliminate the subrange inconsistency? Can we minimise the interpolation errors? And, how do we assess the uncertainty due to the interpolation errors?

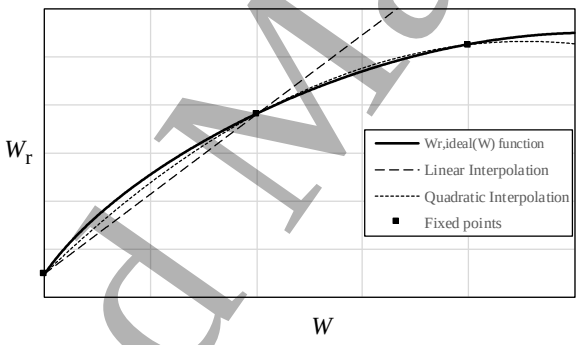


**Figure 2:** Illustration of interpolation error.

Suppose there exists, for each SPRT, a unique, high-order and error-free function, $W_{r,ideal}(W)$, that maps $W(T_{90})$ to $W_r(T_{90})$ exactly for all $T_{90}$ in the range spanned by the interpolation, and captures all the complex behaviour of the SPRT. The interpolation error associated with any of the simpler ITS-90 interpolations, $W_r(W)$, is

$$e(W) = W_{r,ideal}(W) - W_r(W) . \quad (28)$$

Although it is not possible to write down an explicit equation for the interpolation error, the general form of the error is known [31]:

$$e(W) = (W_1 - W)(W_2 - W)(...)(W_N - W)\left[W_{r,ideal}^{(N)}(\xi) - W_r^{(N)}(\xi)\right] / N! , \quad (29)$$

where $N-1$ is the order of the interpolation, the superscript indicates the $N$th derivative with respect to $W$, $W_1 < W_2 < \ldots < W_N$ are the measured $W$ values at the $N$ fixed points, and $\xi$ is some unknown value of $W$ with $W_1 < \xi < W_N$. For any interpolation, there is always a value for $\xi$ such that (29) is true.

Several properties of the interpolation error are apparent from (29):

- the error is zero at each of the calibration points, $W_1 \ldots W_N$,
- the error changes sign at each calibration point giving the error its characteristic oscillatory shape,
- the interpolation error tends to increase in proportion to $\left(W_{\mathrm{H}} - W_{\mathrm{L}}\right)^N$, where $W_{\mathrm{L}}$ and $W_{\mathrm{H}}$ are, respectively, the low and high limits of the interpolation, and
- the interpolation error is zero for all values of $W$ only when $W_{\mathrm{r,ideal}}^{(N)}(W) = W_{\mathrm{r}}^{(N)}(W)$.

The first three points describe the typical characteristics of both NU3 and SRI, examples of which are shown in Figure 3. The last point provides insights into the ideal form of the reference function. Consider the case for Lagrange interpolation, for which $W_{\mathrm{r}}^{(N)}(W) = 0$ always, and therefore the requirement for zero interpolation error is $W_{\mathrm{r,ideal}}^{(N)}(W) = 0$. It follows that for a scale that includes linear interpolations, $W_{\mathrm{r,ideal}}(W)$ should be restricted to linear functions of $W$ and the simplest function satisfying this requirement is $W_{\mathrm{r,ideal}}(W) = W$. That is, if the reference function is identical to the response of the SPRT, $W(T_{90})$, then the interpolation error is zero for all polynomial interpolations. Although this conclusion is obvious, the derivation highlights the importance of choosing a reference function that closely follows the SPRT response to ensure the interpolation error is minimised. Of course, we can only make this identically true for a single SPRT. For a population of SPRTs, the reference function should be chosen to ensure that the average of $W_{\mathrm{r,ideal}}^{(N)}(W)$ is zero for each value of $N$. Because $W_{\mathrm{r,ideal}}(W)$ cannot be known for any SPRT, we cannot design the ITS *a priori* to meet these conditions. The best we can do is test the ITS to ensure the average SRI is zero for every pair of subranges. If the average SRI is zero, the standard deviation of the interpolation errors (NU3) for any subrange becomes a direct measure of the irreproducibility of that subrange.

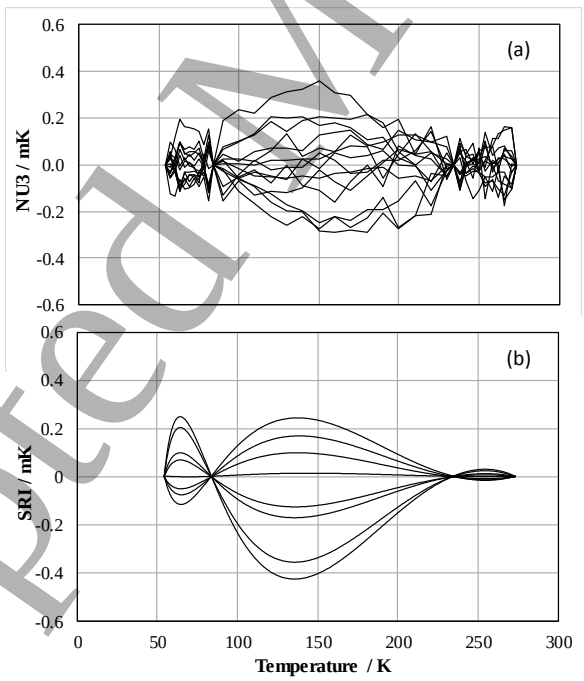


**Figure 3:** (a) NU3 for 14 SPRTs for the oxygen-water subrange, calculated from the data of [42, 43], and (b) SRI between the neon-water and oxygen-water subranges for 8 SPRTs, from the data of [44], illustrating the oscillatory behaviour and zeros at the calibration points.

For non-Lagrange interpolation, the situation is more complicated. Because $W_r^{(N)}(W) \neq 0$ in general for non-Lagrange interpolations, the reference function must be biased away from $W_{r,ideal}(W) = W$ to minimise the interpolation error. Indeed, it is possible that the four interpolations for the ITS-90 subranges below 0.01 °C require four different reference functions to minimise the interpolation error, so that it may be impossible to avoid SRI. Further research is required to understand this situation.

For any SPRT and interpolating equation, there is an interpolation $W_r^*(W)$ that yields the minimum interpolation error,

$$e_{min}(W) = W_{r,ideal}(W) - W_r^*(W). \quad (30)$$

The minimum error can be defined in many ways, including by the least-squares criterion, otherwise known as the Euclidean or $L_2$ norm [31, 33], where $e_{min}(W)$ is the interpolation error when the integral

$$\int_{W_1}^{W_N} [e(W)]^2 \, dW \quad . \quad (31)$$

is minimised. The actual interpolation error, (28), can be rewritten in terms of the minimum error by the following rearrangements [32]. First, (28) is rewritten

$$e(W) = \left[ W_{r,ideal}(W) - W_r^*(W) \right] + \left[ W_r^*(W) - W_r(W) \right]. \quad (32)$$

The first term on the right-hand side of (32) is the minimum error, (30). The second term of (32) is now rearranged using the identity (10) and the fact that $W_{r,ideal}(W) = W_r(W)$ at the fixed points; hence

$$e(W) = e_{min}(W) - \sum_{i=1}^{N} \left[ W_{r,ideal}(W_i) - W_r^*(W_i) \right] F_i(W), \quad (33)$$

or

$$e(W) = e_{min}(W) - \sum_{i=1}^{N} e_{min}(W_i) F_i(W). \quad (34)$$

Since $e_{min}(W)$ is the minimum interpolation error, any quantity added to or subtracted from $e_{min}(W)$ will increase the error (i.e., the second term of (34) is orthogonal to the first term). The actual interpolation error will therefore be greater than the minimum interpolation error by an amount that depends on the interpolating functions, $F_i(W)$, unless the calibration points, $W_i$, coincide with zeros in $e_{min}(W)$.

Equation (34) shows there are two ways of minimising interpolation error. Firstly, by using interpolating equations that closely approximate the true behaviour of the SPRT, thereby ensuring that $e_{min}(W)$ is small. Secondly, by selecting interpolating functions with magnitudes $|F_i(W)| \leq 1.0$ to minimise the amplification of the errors propagated from the $e_{min}(W_i)$ values at the fixed points. For the most part, the interpolating functions of ITS-90 do not exhibit excessive error amplification. However, the interpolations for the argon-water, neon-water and equilibrium hydrogen-water subranges have interpolating functions with values close to 2.0 for some values of $W$ [3, 4, 35] (see also Secs. 2.7 and 3.3.1 below).

The spacing of the calibration points has a strong influence on the error amplification caused by the interpolating functions, and values of $|F_i(W)| > 1.0$ are often associated with oscillatory behaviour (Runge's phenomenon) near the ends of the interpolation interval and poor convergence to the approximated function [33]. For Lagrange (polynomial) interpolation, there is an optimal spacing of the calibration points that minimizes the amplification and optimises the convergence by ensuring $|F_i(W)| \leq 1.0$ for all $W$ within the interpolation range. For an interpolation between the lowest and highest values, $W_L$ and $W_H$, respectively, the calibration points should be spaced according to [31, 33]

$$W_i = \frac{(W_H + W_L)}{2} + \frac{(W_H - W_L)}{2}\frac{\cos\left((2i-1)\pi/2N\right)}{\cos\left(\pi/2N\right)}, \quad i = 1..N\,. \tag{35}$$

This selection of calibration points yields Chebyshev interpolation.

Unfortunately, we cannot place calibration points at will. Instead the location and spacing of the calibration points is set by the physical properties of available fixed-point materials. However, we can select amongst the available fixed-point and interpolation function candidates to ensure that the interpolating functions are well behaved. Another solution may be to subject the *W* values to a monotonic non-linear transformation, say *Y*(*W*), so that the calibration points become correctly spaced for interpolation in the *Y* variable (see Section 3.4.1 for detail).

## 2.6 Subrange Inconsistency

ITS-90 was the first ITS to offer alternative interpolations over some temperature ranges. The differences in calculated temperature due to the use of different equations for the same SPRT are collectively called Type 1 non-uniqueness or subrange inconsistency (SRI) [3, 4, 41, 42]. If we consider two interpolations, ${}^{1}W_{\mathrm{r}}(W)$ and ${}^{2}W_{\mathrm{r}}(W)$, used to approximate the same $W_{\mathrm{r,ideal}}(W)$, then from (28), it follows that

$${}^{1}W_{\mathrm{r}}(W) - {}^{2}W_{\mathrm{r}}(W) = {}^{2}e(W) - {}^{1}e(W)\,. \tag{36}$$

Thus, although the SRI is calculated exactly as a difference in interpolated values, it is also the difference in the (unknown) interpolation errors.

Because the SRI can be expressed exactly in terms of the difference between two interpolating equations, very specific requirements can be determined to ensure subranges are consistent. Consider the difference between the interpolations for the water-tin and water-indium subranges, written in the form [37]

$${}^{\mathrm{Sn}}W_{\mathrm{r}}(W) - {}^{\mathrm{In}}W_{\mathrm{r}}(W) = \frac{(W-1)(W-W_{\mathrm{In}})}{(W_{\mathrm{Sn}}-W_{\mathrm{In}})}\left(\frac{W_{\mathrm{r,Sn}}-1}{W_{\mathrm{Sn}}-1} - \frac{W_{\mathrm{r,In}}-1}{W_{\mathrm{In}}-1}\right). \tag{37}$$

The SRI has zeros at the shared fixed points (water and indium), and is zero for all *W* values when

$$\frac{W_{\mathrm{Sn}}-1}{W_{\mathrm{r,Sn}}-1} = \frac{W_{\mathrm{In}}-1}{W_{\mathrm{r,In}}-1}. \tag{38}$$

Calculations of the SRI for other pairs of interpolating equations show the same features as (37): zeros at the shared fixed points, and a magnitude that depends on the match between parameters of the form

$$S_i = \frac{W_i - 1}{W_{\mathrm{r},i} - 1}. \tag{39}$$

Figure 4 plots the *S* values for a total of 57 SPRTs [37] for several fixed points. Note that *S* has been defined so that it measures the sensitivity of the SPRT relative to the reference resistance ratio, i.e., d*W*/d$W_{\mathrm{r}}$. *S* is the reciprocal of the factor appearing in the SRI equations, e.g., (37).

Remarkably, for long-stem SPRTs, the *S* values are nearly constant across the different fixed points for each SPRT. This is a consequence of platinum resistivity closely following Matthiessen's rule [37],

$$\rho(T) = \rho_{\mathrm{ideal}}(T) + \Delta\rho, \tag{40}$$

where $\rho_{\mathrm{ideal}}(T)$ is the resistivity of pure platinum, and $\Delta\rho$ is a temperature-independent offset caused by impurities and defects. This property means, to good approximation, departures of $W(T_{90})$ functions from the reference function are well modelled by linear interpolations. The same linear behaviour is responsible for the well-known linear correlations between resistance ratios at different fixed points [37, 45-48]. Indeed, the correlation equations are

rearrangements of equations like (38). Figure 4 also shows an interesting effect, perhaps related to the purity and/or diameter of the wire used in SPRTs; the high temperature SPRTs (those calibrated at the silver point), have higher *S* values than those SPRTs designed for lower temperature ranges.

For the SRI to be zero for all pairs of interpolating equations (especially pairs including linear equations), the *S* values for any SPRT should be the same at all fixed points. There are several factors that contribute to variations in *S* for any single SPRT. Firstly, the consistency of the reference resistance ratios assigned by ITS-90 to the different fixed points affects the distribution of measured *S* values. Secondly, variations in the temperatures realized by fixed points due to thermal and impurity effects lead to variations in the $W_i$, and therefore also variations in the *S* values. Finally, all SPRT behaviour is more complex than suggested by Matthiessen's rule, especially at temperatures below 80 K and above 700 °C (see Sec 3.4.2 below).

The effect of inconsistent reference-resistance-ratio definitions is evident in Figure 4, where the *S* values for the mercury point are, on average, too high (i.e., $W_{r,Hg}$ is too small) [37, 45, 46]. To a lesser extent, the *S* values for the argon point also appear high.

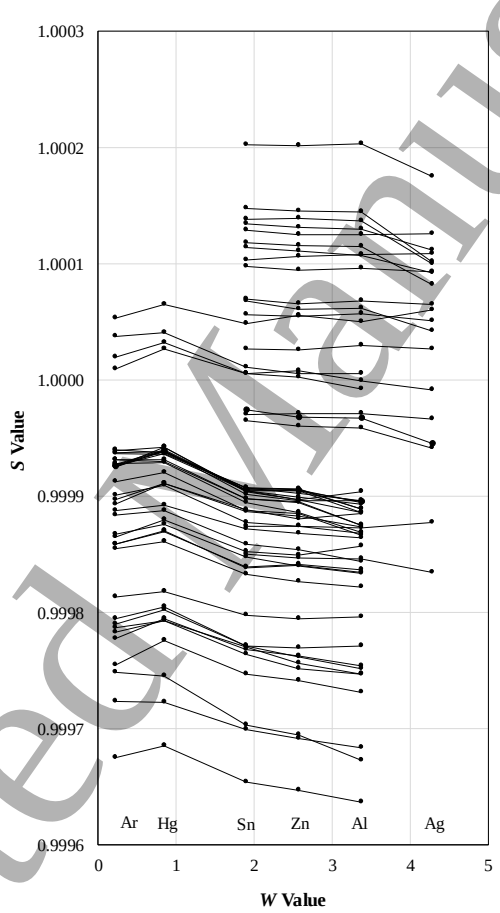


**Figure 4:** The *S*-parameter plot for 57 different SPRTs [37].

For the subranges in the temperature range between the mercury to aluminium fixed points, there are six ITS-90 interpolating equations leading to fifteen instances of overlaps, with each overlap having its own SRI. To date, most studies [37, 49-52] have investigated the SRI between the water-zinc and water-aluminium interpolations, as summarised in the appendix of [53]. The extreme value for the SRI occurs near 93 ºC, and analysis from the five studies yields estimates of the mean maximum SRI ranging from –0.22 mK to +0.23 mK, while the mean of all studies is 0.1 mK. Certainly, for these two subranges, the average SRI is negligible compared to the interpolation error itself. The standard deviations of the peak SRI for each of five studies fall between 0.29 mK and 0.48 mK

[53], which is of a similar magnitude to the uncertainties in the fixed-point realisations reported in the BIPM key-comparison database.

For temperatures below 0.01 °C, the most recent substantive studies are by Steele [54] and by Meyer and Tew [44], who considered the SRI between the four lowest SPRT subranges of ITS-90 spanning 13.8 K to the TPW. The data set of Steele is constructed from the calibrations of 13 SPRTs used in the CCT-K2 key comparison [55]. Meyer and Tew report the results for 18 SPRTs and describe efforts to include thermometers spanning extremes of characteristics. Meyer and Tew calculate the standard deviation of SRI over their SPRT ensemble for each subrange relative to the average of all four subranges, but neither study reports the mean SRI (subrange bias) values of their respective ensembles. A re-analysis of the data of Steele, following the approach of Meyer and Tew but with the addition of mean SRI curves, is plotted in Figure 5. The resulting SRI standard deviations are similar to those of Figure 10 from [44]. For all four subranges, the mean SRI is always less than the standard deviation, and mostly below 0.05 mK. However, the mean SRI between the *e*-$H_2$ to TPW and Ne to TPW interpolations is larger than desirable below 54 K, peaking to 0.23 mK at 30 K, likely due to the poor interpolation of the Ne to TPW subrange at these temperatures (see Sec. 2.7).

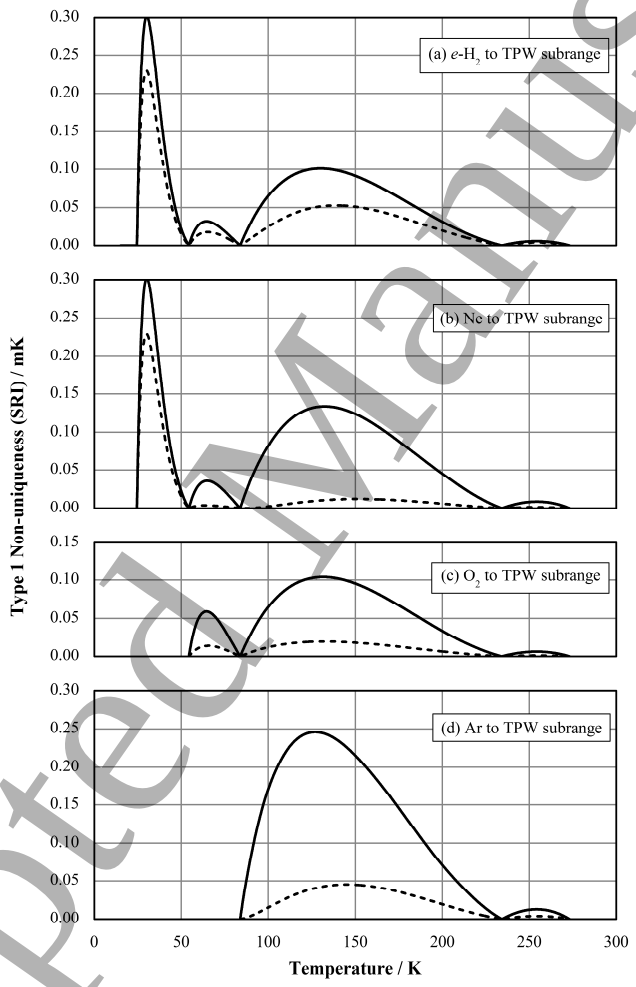


**Figure 5:** Subrange inconsistency from the CCT-K2 calibration data, calculated from the data of [54, 55], for the (a) *e*-$H_2$ to TPW subrange, (b) Ne to TPW subrange, (c) $O_2$ to TPW subrange, and (d) Ar to TPW subrange. The dotted lines show the absolute values of the mean SRI and solid lines show the standard deviations of the SRI for each subrange relative to the average of all four subranges.

## 2.7 NU3 Uncertainty in ITS-90

As explained in Section 2.5, if the average SRI between different interpolations is close to zero, the uncertainty in the scale temperatures due to interpolation error can be calculated simply as the standard deviation of the interpolation errors for a group of SPRTs, i.e., Type 3 non-uniqueness (NU3). This conclusion is consistent with the recommendations of Rusby *et al* [53], but different to that recommended in [35, 42], which suggests combining the uncertainties due to NU3 and SRI. A useful consequence of the conclusion and Rusby's recommendation is that subranges can be added to ITS-90 without compromising the uncertainty of other subranges, so long as the interpolations used in the new subranges do not introduce significant SRI. Some possibilities are considered in Sec. 3.5.

In the temperature range between 0 ºC and 962 ºC there is limited data on NU3 because of problems with platinum oxidation and drift of SPRTs, and historical studies have focused on the water-zinc, water-aluminium, and water-silver subranges. Most data are drawn from calibrations at redundant fixed points [56-60]. In all cases, the uncertainties include uncertainties propagated from the calibrating fixed points, oxidation effects, resistance measurements, and non-uniformity of the comparison media. Thus, studies reporting the lowest values at any point are likely to provide the best estimate of the contribution of the non-uniqueness. Figure 6 plots the representation of the NU3 given in [35, 42], which uses four parabolic curves to indicate the magnitude of the NU3. New, highly precise measurements in a stirred oil bath suggest an upper limit for NU3 of 0.03 mK from -38 °C to 30 °C, and 0.1 mK from -95 °C to 80 °C [61]. The NU3 for the water-tin and water-indium subranges is unknown.

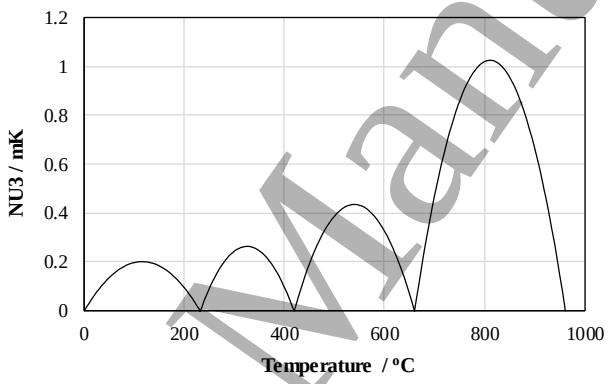


**Figure 6:** Estimate of Type 3 non-uniqueness of ITS-90 for water-zinc, zinc-aluminium, and aluminium-silver ranges, from [35, 42].

In the range from the triple point of equilibrium hydrogen at 13.8 K to the triple point of water at 273.16 K, the most recent estimate of NU3 comes from the standard deviation of comparison block measurements performed at NRC [43]. This data set was analysed in [42] using the *e*-$H_2$ to TPW interpolation but truncated at the triple point of neon (24.5 K). The resulting NU3 data are shown in Figure 7 (a). Figure 7 also restores the NU3 data below 24.5 K, along with points analysed using the Ne to TPW, $O_2$ to TPW and Ar to TPW interpolating equations, which had been omitted from [42]. Despite using different ensembles of SPRTs (CCT-K2 data are not included in the NU3 data set due to measurement protocol deficiencies described in [43]), the standard deviation of NU3 data shown in Figure 7 and standard deviation of SRI data shown in Figure 5 are very similar. Figure 7 shows that NU3 is less than 0.2 mK or so for most of the subranges below the TPW, but there are three exceptions where the interpolating functions are known to amplify uncertainties: the *e*-$H_2$ to TPW interpolation below 17 K, the Ne to TPW interpolation below 54 K, and, to a lesser extent, the Ar to TPW interpolation between 100 K and 200 K.

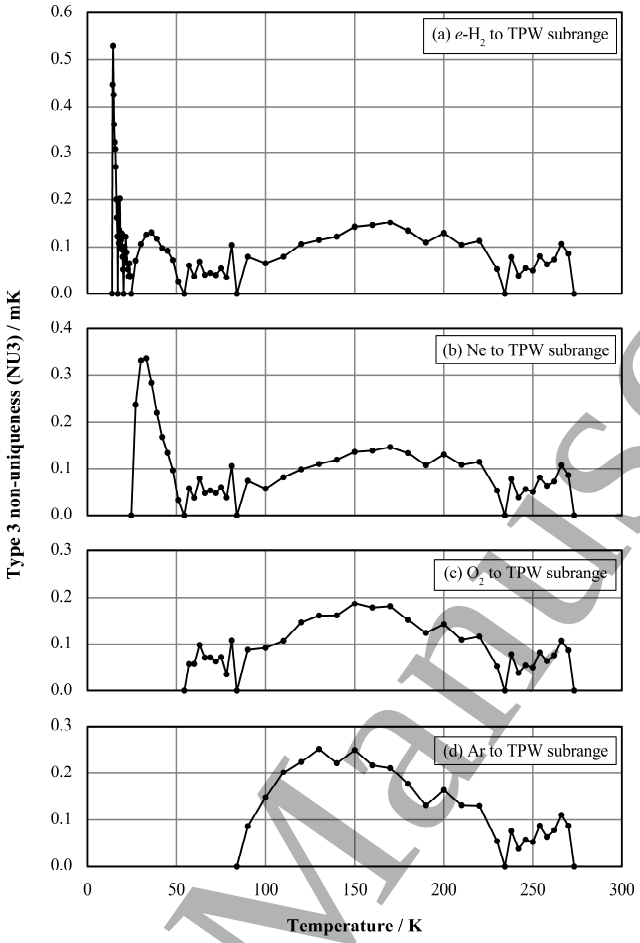


**Figure 7:** Uncertainty of the ITS-90 due to Type 3 non-uniqueness (NU3), calculated as standard deviations, in the temperature range 13.8 K to 273.16 K. The data have been adapted and extended from [42, 43], and are shown for the (a) *e*-$H_2$ to TPW subrange, (b) Ne to TPW subrange, (c) $O_2$ to TPW subrange, and (d) Ar to TPW subrange.

## 2.8 Discontinuity at the triple point of water

Rusby [62] reported evidence for a small but statistically significant discontinuity in the first derivative of ITS-90 at the triple point of water. The origin of the discontinuity can be identified by considering the derivative $\partial T_{90} / \partial T$ [63]:

$$\frac{\partial T_{90}}{\partial T} = \frac{\partial T_{90}}{\partial W_{\mathrm{r}}} \times \frac{\partial W_{\mathrm{r}}}{\partial W} \times \frac{\partial W}{\partial T} \,. \qquad (41)$$

The first term on the right hand side of (41) is simply the derivative of the reference function defined by ITS-90. Although defined in two segments, by design the function has continuous first and second derivatives so cannot be the source of the discontinuity [3, 4]. The third term of (41) is proportional to $\partial R / \partial T$ , which is a physical property of an individual SPRT. We can also assume this to be continuous in the first derivative, and certainly it is very unlikely for any discontinuity to occur at 0.01 ºC exactly.

The second term of (41) is the derivative of an ITS-90 interpolating function, and the origin of the discontinuity. While all the interpolations are demonstrably continuous within their respective subranges, first-order discontinuities occur where subranges terminate and meet, i.e., at the triple point of water. Note that there is no

discontinuity at the triple point of water if only the mercury-gallium subrange is used to calculate temperatures immediately above and below the triple point of water.

Additional insights into the origin of the discontinuity can be gained by rearranging the ITS-90 interpolations in terms of $S = (W-1)/(W_r-1)$ rather than resistance ratio. For example, the quadratic ITS-90 interpolation for the mercury-gallium subrange is

$$W_r = W_{r,Hg}\frac{(W-1)(W-W_{Ga})}{(W_{Hg}-1)(W_{Hg}-W_{Ga})} + \frac{(W-W_{Hg})(W-W_{Ga})}{(1-W_{Hg})(1-W_{Ga})} + W_{r,Ga}\frac{(W-1)(W-W_{Hg})}{(W_{Ga}-1)(W_{Ga}-W_{Hg})}. \quad (42)$$

With the help of (18), this can be rewritten

$$\frac{W_r-1}{W-1} = \frac{(W_{r,Hg}-1)}{(W_{Hg}-1)}\frac{(W-W_{Ga})}{(W_{Hg}-W_{Ga})} + \frac{(W_{r,Ga}-1)}{(W_{Ga}-1)}\frac{(W-W_{Hg})}{(W_{Ga}-W_{Hg})} \quad (43)$$

or

$$\frac{1}{S} = \frac{1}{S_{Hg}}\frac{(W-W_{Ga})}{(W_{Hg}-W_{Ga})} + \frac{1}{S_{Ga}}\frac{(W-W_{Hg})}{(W_{Ga}-W_{Hg})}. \quad (44)$$

Thus, the quadratic interpolation of $W_r$ values is a linear interpolation of $1/S$ values. For all ITS-90 interpolations, an $n^{th}$ order interpolation of $W$ values is equivalent to an $n-1^{th}$ order interpolation of $1/S$ values.

Figure 8, which plots several of the ITS-90 interpolations for a single SPRT, now shows the origin of the discontinuity more clearly. ITS-90 interpolations that are linear in $W$ (water-gallium or water-indium) on this graph are horizontal lines, and quadratic ITS-90 interpolations (e.g., mercury-gallium) are straight lines with slopes. The points where the lines intersect with the vertical $W = 1$ line give the value

$$\left.\frac{(W_r-1)}{(W-1)}\right|_{W=1} = \left.\frac{dW_r}{dW}\right|_{W=1}. \quad (45)$$

Thus, wherever the points of intersection at $W = 1$ give different values, there will be discontinuities in the derivative of ITS-90 when changing from one interpolation equation to another. Figure 4 shows that for any SPRT, the $S$ values below $W = 1$ are all higher than the $S$ values above $W = 1$, so that there is a consistent discontinuity in $dT_{90}/dT$ at the triple point of water. Thus, the discontinuity is linked to the poor choices of reference resistance ratios assigned to the fixed points and therefore also to SRI. The discovery of the discontinuity reinforces the case (Sec. 3.2.1) for making the reference resistance ratios more consistent.

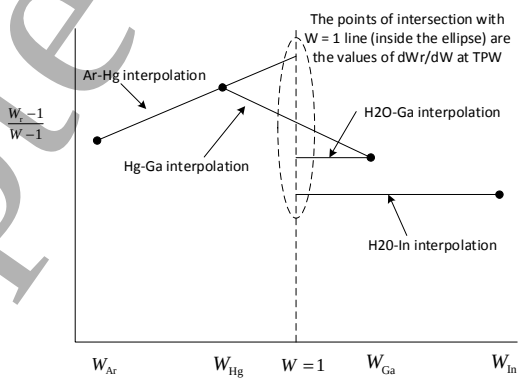

**Figure 8:** The different ITS-90 interpolations for a single SPRT plotted as interpolations of 1/*S*. The points of intersection of each of the interpolations with the vertical $W = 1$ line indicate the derivative of $dW_r/dW$ at the triple point of water for that interpolation.

## 2.9 Separation of Reproducibility and Accuracy

As the sections above show, the uncertainty propagated from fixed-point realizations, resistance measurements, and NU3 all contribute to the dispersion of calculated $W_r$ values, and hence to the inherent irreproducibility of $T_{90}$. In contrast, the last ITS-90 transformation, $T_{90}(W_r)$, is exact and one-to-one so cannot introduce any additional uncertainty into ITS-90. That is, the transformations $R \rightarrow W \rightarrow W_r$ are entirely responsible for the irreproducibility/uncertainty of $T_{90}$ values, and the $W_r \rightarrow T_{90}$ transformation, embodied in the reference function, is responsible for the thermodynamic accuracy of ITS-90. Because the attributes of reproducibility and accuracy of the temperature scale are separable in this way, no compromise between the two properties is necessary. This observation also explains why a proposed reformulation of the ITS-90 reference function to improve the thermodynamic accuracy made no improvement to the uncertainty [64].

The separation of the scale reproducibility and accuracy means that scale development should be carried out in two steps. Firstly, interpolating functions, fixed points, and reference resistance ratios should be chosen to minimize the dispersion of interpolated $W_r$ values. Then, once highly reproducible $W_r$ values have been obtained, they can be mapped to $T_{XX}$ using an appropriate $W_r(T_{XX})$ function to minimize $T - T_{XX}$. If a complete ITS overhaul is desired, it is important that the scale is constructed in this sequence, *i.e.*, the fixed-point temperatures and reference resistance ratios must be assigned independently, and only coupled at the last step when $W_r(T_{XX})$ is determined.

# 3 OPTIONS FOR REVISON

## 3.1 Clarifications

ITS-90 has a few minor causes of confusion that could usefully be removed. The changes suggested here have little consequence for almost all users of the scale, and most can be put into practice simply by including them in the technical annex to the ITS-90 [65].

### *3.1.1 The $W_r(T_{90})$ overlap*

At present the two segments of the $W_r(T_{90})$ reference function overlap between 0.0 °C and 0.01 °C. Although the overlap causes negligible differences in calculated temperatures, it is a source of confusion and is an unsightly artefact that can be removed by making the endpoint of both segments 0.01 °C. If changed, some existing documentation and CMC definitions might have to change. No scientific research is required to support this change.

### *3.1.2 Hg and Ga SPRT Quality Criteria*

Currently, the ITS-90 SPRT quality criteria, based on the measured resistance ratios at the gallium point ($W_{Ga} \geq 1.11807$) and the mercury point ($W_{Hg} \leq 0.844235$) are inconsistent and confusing because it is possible for SPRTs to clearly meet the mercury-point criterion but, just as clearly, fail to meet the gallium-point criterion. The least confusing solution is to use a single criterion, and given the possible problems with mercury, the gallium-point criterion would be the better of the two. This solution relies on the ready availability of gallium cells with sufficiently wide thermometer wells to accommodate both capsule SPRTs and long-stem SPRTs.

An alternative is to have a criterion based on the *S* parameter (39) and applicable to any fixed point in the range from the argon point to the aluminium point. The corresponding *S* values for the current ITS-90 gallium- and mercury-point criteria are 0.999 417 and 0.999 404 [37], so a single general criterion such as

$$S_i = \frac{W_i - 1}{W_{r,i} - 1} > 0.99941, \qquad (46)$$

could usefully replace the current two criteria. The use of the general criterion would substantially reduce the ambiguity and offer greater flexibility for calibration procedures.

Research is required to refine the value of *S* for the qualifying criterion. For example, all 57 of the long-stem SPRTs represented in Figure 4 demonstrably satisfy $S_i > 0.9996$, suggesting the current criteria are not very discerning. However, the *S* values for some capsule thermometers are lower than those for long-stem SPRTs (see Sec. 3.4.2 below).

*3.1.3 Ag SPRT qualification criterion*

The quality criterion at the silver point, $W_{Ag} \geq 4.2844$ (equivalent to $S_{Ag} \geq 0.999385$), is intended to disqualify high temperature SPRTs exhibiting large electrical-insulation breakdown effects [66]. At the time the ITS-90 was formulated, the mechanism of the insulation breakdown was not understood. The effects are now thought to be caused by electrical leakage through metal-semiconductor (a.k.a. Schottky or point-contact) diodes formed between the fused-silica insulators and the platinum wire [67, 68], and then by ionic conduction through the fused-silica insulators. In effect, the quality criterion should select for SPRTs with the highest-purity insulators.

In Figure 4, about half of the high-temperature SPRTs show a distinct fall in *S* value between the aluminium and silver points, with the differences corresponding to errors of up to 40 mK at the silver point. Although the cause of the differences is not known, the temperature of occurrence, magnitudes, and signs of the differences are consistent with electrical leakage effects. However, all the SPRTs in Figure 4 easily satisfy $W_{Ag} \geq 4.2844$, and it seems very unlikely that any SPRT meeting the mercury or gallium criteria has ever been disqualified due to a poor resistance ratio at the silver point. Further, there is no single value of $W_{Ag}$ that would usefully distinguish good SPRTs from SPRTs with a significant electrical leakage problem. These observations suggest that the silver-point quality criterion serves no purpose and should be withdrawn.

Recent work by Widiatmo *et al* [69], building on earlier work by several researchers summarised in [67], has shown that the application of a small dc voltage between the SPRT sensing element and the sheath during measurement reverse biases the Schottky diodes and switches off the non-linear conduction path through the diodes and the fused silica, leading to higher and more consistent values of measured resistance for both ac and dc measurements. This suggests the way forward is to replace the silver-point quality criterion with an assessment of uncertainty due to electrical leakage effects. The uncertainty estimate could be supported either by the measurement of the change in resistance that occurs with the application of the bias voltage, or by the measured difference in the *S* values for the aluminium and silver points.

Research is required to establish appropriate procedures for the assessment of uncertainty due to electrical leakage. First, the results of Widiatmo *et al* should be reproduced at different laboratories, using different resistance bridges, with different silver-point cells, in different furnaces, and with different temperature profiles along the SPRT (since the lead wires and their insulators contribute distinct leakage paths). If it can be confirmed that the bias voltage indeed makes the resistance measurement insensitive to the leakage effects, the resistance of SPRTs at high temperatures can be defined to be with the bias voltage applied.

Secondly, it would be helpful to establish a model of the temperature dependence of the leakage effects by repeating the measurements of the leakage effect at temperatures other than the silver point. It may be that the model developed by White *et al* [67] for a single platinum-silica Schottky diode is a satisfactory description of many such diodes in parallel. The model would provide a basis for propagating uncertainties measured at the silver point to lower temperatures. Thirdly, it would be helpful to confirm that the *S*-parameter differences between the aluminium and silver points seen in some of the SPRTs of Figure 4 are indeed due to leakage effects, and if so, to correlate the magnitude of leakage effects with the observed differences in *S* values.

*3.1.4 Use NU3 to characterise scale uncertainty*

The discussion of Section 2 shows that, so long as the average SRI for all overlapping pairs of subranges is close to zero, the contribution of interpolation error to scale uncertainty is determined solely by the NU3 for the subrange in use. This conclusion suggests several changes to normal practice.

First, the technical annex to the ITS-90 [65] or the *Guide to the Realization of the ITS-90* [42] should clarify the interpretation of the 'equal status' of the various subranges by (i) stating that SRI is simply an alternative manifestation of NU3 and there is no need to include it in any calculation of the uncertainty in $T_{90}$, and (ii) endorsing the perspective that while all subranges produce equally valid measurements of $T_{90}$, the subrange with the lowest uncertainty yields the best measurements of $T_{90}$.

Secondly, there would be an immediate reduction in the current best estimates of the uncertainties in $T_{90}$ due to the removal of the contribution due to SRI. Notably, subranges with low values of NU3 have much lower uncertainties than previously indicated. The updated estimates should be included in the *Guide to the Realization of the ITS-90*.

Finally, substantial research into interpolation error is required to support both ITS-90 and any future scale development. In particular, there are subranges above 0.01 °C for which there are no measurements of NU3. It should also be confirmed that the average SRI for all pairs of subranges is not significantly different from zero. Measurements used to calculate NU3 and SRI for ITS-90 can also be used to determine the NU3 and SRI for a future scale.

## 3.2 New Reference Function

The 2011 report of the CCT Working Group 4 (now the Working Group on Contact Thermometry) [70] concluded that there are substantial differences between ITS-90 scale temperatures and thermodynamic temperatures, as shown in Figure 9. Recent measurements of $T–T_{90}$ have largely confirmed the 2011 summary [71-75], and significantly lowered the uncertainties in some of the differences. These differences are the most obvious and most easily fixed shortcomings of ITS-90. As noted in section 2.9, the improved accuracy must be embodied in a new reference function.

Although the SRI is negligible for most pairs of overlapping subranges, there is room for improvement with the low temperature subranges. Also, there is an opportunity to reduce the discontinuity at the triple point of water. These improvements also require a new reference function. Thus, there are two reasons for revising the reference function, one to improve its thermodynamic accuracy, the other to improve the reproducibility and continuity.

In principle, a new reference function could take any form. However, Hill & Steele recognized that from an engineering perspective, the simplest substantial change that could be made to ITS-90 is to improve thermodynamic accuracy by changing the values of the constants defining the reference function, $W_r(T_{90})$, without changing its functional form [76, 77]. Such a change might have a minor effect on software in commercial instrumentation, perhaps only affecting tables of constants, and may be less disruptive than changes to the underlying mathematical structure of the reference function.

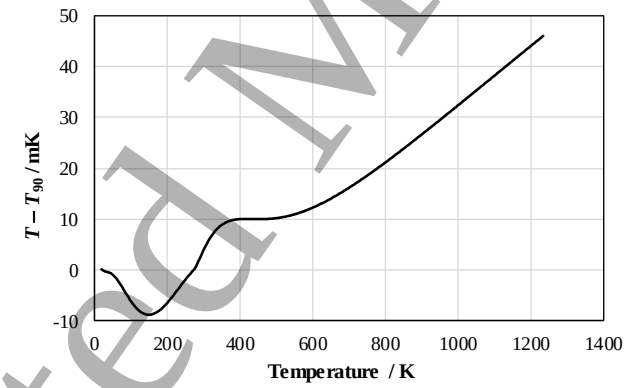


**Figure 9:** Current estimates of the temperature differences $T - T_{90}$ [70].

*3.2.1 Optimisation of reference resistance ratios*

As discussed in Sections 2.6 and 2.8, the discontinuity in $dT_{90}/dT$ at the TPW and some of the SRI arises from the inconsistent values of the reference resistance ratios, $W_{r,i}$, assigned to the fixed points. It is possible to improve the SRI by adjusting the $W_{r,i}$ values to ensure greater consistency, while leaving ITS-90 substantially unchanged. This requires (i) a process to adjust the $W_{r,i}$ values to minimise SRI and the TPW discontinuity, and (ii) the development of new coefficients for the $W_r(T_{90})$ function to ensure scale temperatures assigned to the fixed points do not change with the new $W_{r,i}$ values and that other scale temperatures do not change significantly. While some tweaks for the same purpose were made during the construction of the ITS-90 [46, 66], the resulting $W_{r,i}$ values remained largely

based on data from a single SPRT in each of the two ITS-90 reference function segments, and, as shown in Figures 4 and 14, are not representative of the population of SPRTs.

Substantial research is required before the changes should be considered. Firstly, it is necessary to collate high-quality fixed-point measurements for many SPRTs, of all makes and models and spanning all fixed points. Once the data is collated, a least-squares adjustment can be performed to adjust the $W_{r,i}$ values so that on average, the $S_i$ values for any individual SPRT are as similar as possible. A weighted adjustment could be employed to minimise SRI in important temperature ranges.

Fixed-point measurements below the argon point should probably be omitted from the adjustment because Matthiessen's rule, (40), which underpins the constant *S*-parameter behaviour observed in Figure 4, breaks down at lower temperatures (see Section 3.4.2 below). If the use of a bias voltage for supressing electrical leakage effects at the silver point proves to be effective, then only silver-point measurements made with the bias voltage applied (see Sec. 3.1.3) should be included in the adjustment.

Figure 10 shows the results of a least-squares adjustment for the 57 SPRTs of Figure 4. The adjustment minimised the standard deviation of the *S* value for each SPRT, averaged over all SPRTs and averaged over all fixed points except for the silver point. The optimisation for the silver point was based on five SPRTs for which the ITS-90 values of $S_{\mathrm{Al}} - S_{\mathrm{Ag}}$ were consistent. The adjustment reduced the standard deviation of the *S* values by more than 60%. Much of the reduction arises from the elimination of the discontinuity in *S* values between temperatures above and below 0.01 °C. Nevertheless, this result and Figure 10 show that a useful reduction in SRI is achievable.

An adjustment using the standard deviation of the *S* values effectively fits the equation $S = constant$ to all SPRTs (i.e., assumes linear interpolation in *W* – see Sec. 2.5). It is noticeable in Figure 10 that some of the SPRTs are better modelled by a straight line with a slope (equivalent to a quadratic interpolation in *W*). Thus, the minimisation of the standard deviation of residuals to a straight-line fit might further reduce the SRI for pairs of higher-order interpolations.

Once all the changes have been evaluated, a new scale closely replicating the ITS-90, but with a reduced SRI and negligible discontinuity at the triple point of water, could be promulgated. The changes can probably be made without incurring changes in scale temperature of more than a few tenths of a millikelvin, *i.e.* less than the current scale uncertainty. To most users, the new scale would be indistinguishable from ITS-90 and the consequential costs to instrument manufacturers, standardising organisations etc, would be practically zero, since the new and old scales can coexist, with the new scale being necessary only for the highest accuracy applications.

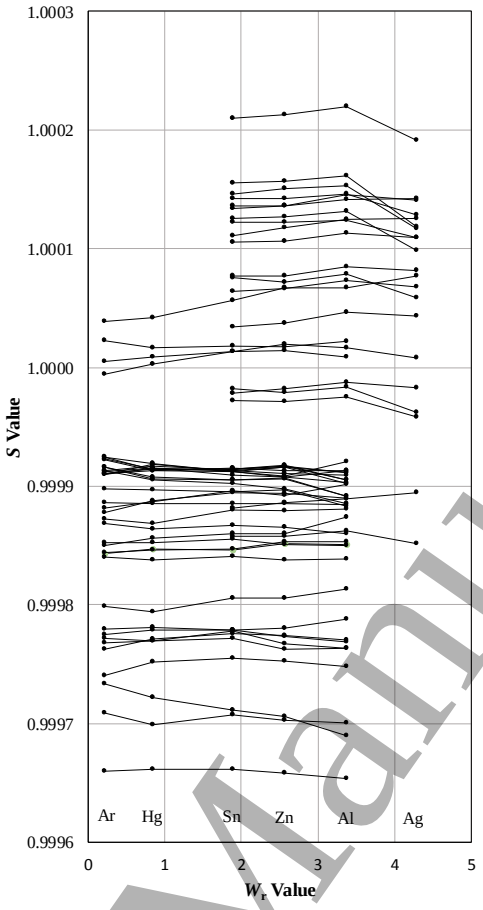


**Figure 10:** An *S*-parameter plot for the 57 SPRTs of Figure 4 [37] with the reference resistance ratios for the fixed points adjusted to minimise the dispersion of *S* values for each SPRT.

*3.2.2 Improved Thermodynamic accuracy*

If the thermodynamic accuracy of the ITS is to be improved, then there is no alternative to revising the reference function. Because the reference resistance ratios at the fixed points must be altered, it makes sense to optimise the $W_{r,i}$ values to minimise SRI first, as described in the previous section. Once the reference resistance ratios for the fixed points have been assigned, thermodynamic temperatures can be assigned to the fixed points and to intermediate temperatures, and a new $W_r(T_{XX})$ function developed.

Over the next five to ten years we should expect greater effort directed to low-uncertainty determinations of $T - T_{90}$. Already, results spanning the range from about 7 K to 330 K and with uncertainties of 1 mK or lower have been published [71-75, 78]. Changes to the scale should be based on the consensus estimate of $T - T_{90}$ prepared by the Contact Thermometry Working Group of CCT in one of its periodic reviews.

Figure 9 shows that the changes in scale temperature would be significant for many users, exceeding 10 mK at temperatures above 100 °C. Such changes would disrupt users who are unconcerned with thermodynamic accuracy but do require an unchanging and highly reproducible temperature scale. For example, a change of only 3 mK at room temperature will affect ultra-precision manufacturing [79]. On the other hand, as direct dissemination of thermodynamic temperature becomes more commonplace, we should expect greater confusion between $T$ and $T_{90}$ (or $T_{XX}$) and updating the ITS to minimize $T - T_{XX}$ would reduce the costs of confusion. Of course, calibration certificates should always clearly indicate whether the calibration is with respect to thermodynamic or scale temperature.

## 3.3 New Fixed-Points

The emerging problems with transport and use of mercury lead naturally to considerations of changes to the selection of fixed points. Direct replacements are an interesting option because the number of fixed points and mathematical formalism in any given subrange might stay the same as in the ITS-90. Thus, like the changes described in the previous section, the scale changes arising from fixed point replacements could be purely numerical.

Extensive research is required to evaluate the quality and availability of any new fixed-point substances, along with the ease of use and reproducibility of the fixed points, how they might be introduced into the temperature scale, and the effects on the interpolating equations and NU3. Once new fixed points are deemed suitable, there can be significant adoption costs related to purchasing, commissioning, and training for both the realisation technique and the associated equipment, redevelopment of technical procedures, participation in comparisons, and the costs of accreditation and regaining recognition of Calibration and Measurement Capabilities (CMCs). It might also be necessary to consider international comparisons of the new fixed points before implementation of a new scale.

*3.3.1 Replace the Mercury point*

There are good reasons for removing or replacing the mercury point, from both logistical and numerical standpoints [80, 81]. Simply removing the mercury point from the ITS, leaving no fixed point between the argon point and TPW, was considered during the development of the ITS-90 and was rejected because NU3 becomes unacceptably large [66] for some subranges. At the same time, the proximity of the mercury point to the triple point of water means that the spacing of the calibration points is far from optimal, leading to excessive amplification of uncertainty and larger than ideal non-uniqueness for other subranges.

Both sulphur hexafluoride, $SF_6$, with a triple point near 223.556 K (−49.596 °C) [82-84], and xenon, with a triple point near 161.406 K (−111.744 °C) [80, 81, 85], show promise as a replacement for mercury. Carbon dioxide, $CO_2$, with a triple point near 216.592 K (−56.558 °C) [86, 87], is another candidate. The use of xenon, instead of mercury, was considered during the development of the ITS-90, but poor reproducibility of the xenon point was then a significant problem [66]. Recent work reveals that krypton impurities were the dominant source of the irreproducibility, and xenon with low krypton content is now available [80, 81, 85].

There are some minor cost-saving opportunities with some of the replacements. The equipment for realizing the xenon point may resemble that for the argon point, whereas the equipment for $SF_6$ and $CO_2$ may share similarities to that for the mercury point. Research is in progress to develop large $SF_6$ cells suitable for the calibration of long-stem SPRTs, perhaps using existing equipment for mercury fixed points [83, 88]. Early work indicates that these large immersion-type cells must be melted using a novel quasi-adiabatic step melting protocol to obtain reproducible results [83] in agreement with those of smaller adiabatic-type cells [82-84].

Figure 11 shows the interpolating functions for the argon-water subrange with (a) the mercury point, as in the current ITS-90, (b) mercury replaced by $SF_6$, and (c) mercury replaced by xenon, with all plots using the current ITS-90 argon-water interpolating equation. The solid lines in the figure show the quadrature sum of the interpolating functions as an indicator of the total uncertainty propagated from the fixed points. The xenon point is an almost perfect replacement for mercury for this subrange, yielding a factor of two reduction in the propagated uncertainty, and possibly a similar reduction in non-uniqueness. This subrange spans the increasingly important range from −110 °C to −70 °C involved with the storage of blood products and tissue samples [89]. The improvement in uncertainty is not as great for the other ITS-90 subranges that currently use mercury: between the argon and mercury triple points, the propagated uncertainty of the *e*-hydrogen-water, neon-water and oxygen-water subranges is estimated to be reduced by 20 % to 30 %, and the NU3 of the *e*-hydrogen-water subrange is reduced by 30 % [85].

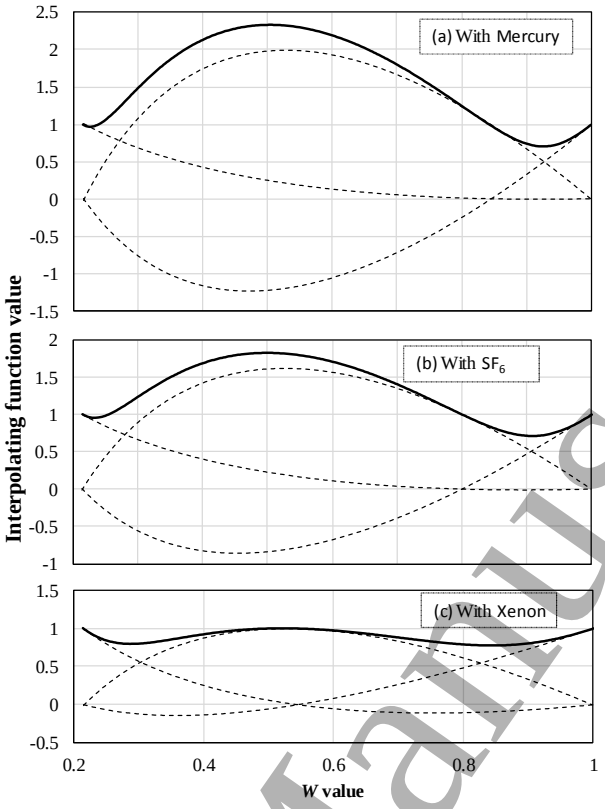


**Figure 11:** Uncertainty propagation for the argon-water subrange (a) with the mercury point (ITS-90), (b) with $SF_6$ replacing mercury, and (c) with xenon replacing mercury. The dotted lines are the interpolating functions, and the solid lines are the quadrature sums of the interpolating functions.

Substantial research is required to support the replacement of the mercury point. The reproducibility of the xenon point has already been demonstrated with a comparison of cells [85], although further measurements are desirable, and the continued availability of commercial xenon gas of sufficient purity, preferably from at least two suppliers, must be confirmed. Work is also required to determine the best $W_{r,i}$ value to assign, and ideally, this process should be as described in Sec. 3.2.1. Work on the design and validation of fixed-point cells and supporting equipment for realizing the new fixed points for long-stem SPRT calibration is also required. This has begun for $SF_6$ [83, 88], whereas for xenon, conversion of existing argon fixed-point apparatus could be explored.

Once the suitability of the fixed points has been established, it is necessary to quantify the effects on the interpolating equations, subrange inconsistency and non-uniqueness of the scale. Understanding the uncertainty propagation is a relatively simple task using (5) and (15), as illustrated in Figure 11, but the non-uniqueness and SRI investigations require access to high-quality temperature-resistance data for a broad sample of SPRTs, and at present we are reliant on the modest sample of capsule SPRTs represented in comparison measurements performed immediately following CCT-K2 [42, 43, 85] (see also Section 2.7).

*3.3.2 Replace the vapour-pressure points*

A significant barrier to the realisation of the SPRT subrange of the ITS-90 extending below 24.5 K is the requirement to realise either the hydrogen vapour-pressure points near 17 K and 20.3 K or an interpolating gas thermometer (4.2 K to 24.5 K subrange with helium-4) at the same temperatures. These two calibration points were retained from the International Practical Temperature Scale of 1968 (IPTS-68) in order to capture the divergence of SPRT characteristics at low temperatures, although soon after the formulation of the ITS-90 it was realised that the positions of these points are not ideal in terms of propagation of uncertainty [3, 4]. The *e*-$H_2$-TPW subrange has the

lowest NU3 of the SPRT subranges over a broad temperature range below 0.01 °C (see Sec. 2.7). However due to the difficulty of realising the 17 K and 20.3 K points, it is rarely used. Rhodium-iron resistance thermometers calibrated in interpolating gas thermometers are sometimes employed as high-quality transfer standards, but this approach has become limited due to lack of availability of new rhodium-iron thermometers of suitable quality. There are several scenarios that might lead to an elimination of the need for the 17 K and 20.3 K points.

It may be that the two points can be replaced by a single equilibrium deuterium triple point, near 18.7 K [90, 91]. A modest investment in a new fixed point compatible with all other cryogenic fixed points would allow the retirement of a complete experimental system. However, a modification of the *e*-$H_2$-TPW deviation function will also be required, and an unacceptable level of NU3 may be incurred [91]. The deuterium triple point is also particularly sensitive to hydrogen impurities (as $H_2$ and HD), posing practical challenges during cell filling and with the long-term stability due to the possible diffusion out of the metallic inner walls of the cells [91]. Substantial research would be required to establish the suitability of the deuterium point, including consideration of hydrogen impurity issues, determination of an appropriate reference resistance ratio, and the development of low-uncertainty interpolating equations to replace the current equations.

It is possible that an improved interpolating equation (Sec. 3.4) might allow the omission of the 17 K and 20.3 K points without the need for any replacement fixed points. This could take two forms, either a new interpolating equation for the whole hydrogen-water subrange (essentially an improved version of the present ITS-90 neon-water subrange, since it already includes an out-of-range calibration point at the *e*-$H_2$ triple point), or a new hydrogen-argon subrange with a much simpler interpolation. Because commercial SPRT-based thermometers with integrated readout electronics are rarely used below the argon point, both options might not be particularly disruptive.

It is also worth considering a scenario in which direct dissemination of thermodynamic temperature overtakes dissemination of the ITS below 24.5 K. In such a case, the simplest approach would be to apply the ITS-90 Ne-TPW subrange for SPRT calibrations above 24.5 K. Unfortunately, in the present ITS-90 formulation, the NU3 of this subrange is significantly larger than that of the *e*-$H_2$-TPW subrange between the triple points of neon and oxygen (Sec. 2.7). It is possible that improved interpolating equations for the Ne-TPW subrange may alleviate this problem too. Alternatively, a primary thermometer used for thermodynamic temperature realization below 24.5 K could also be operated in “interpolating” mode, as has already been done with dielectric constant gas thermometry [12], so that a separate interpolating gas thermometer system is not needed. The option of mimicking hydrogen vapour-pressure calibration using a non-interpolating primary thermometer and consensus $T - T_{90}$ values for the two hydrogen vapour pressure points could also be explored.

*3.3.3 Replace the silver point*

There are practical difficulties working with the silver point due to the high mobility and vapour pressure of silver. The diffusion of silver through the fused-silica sheaths of SPRTs leads to contamination of the platinum sensing element, along with contamination and premature failure of other fused-silica elements of the fixed-point assemblies. Silver fixed points are also susceptible to the effects of dissolved oxygen [92]. The use of SPRTs up to the gold point has been considered in the past, and perhaps now with a better understanding of electrical leakage effects, the gold point could be considered as an alternative to the silver point, simultaneously eliminating the problems with silver and extending the SPRT temperature range by 100 °C [93].

A substantial amount of research is required before such a change could be considered. In addition to the issues around the scale reproducibility and accuracy, successful management of the electrical leakage effects in SPRTs, which increase exponentially with temperature, would also need to be demonstrated. The increased migration of potential contaminants is also a concern [94], although there is evidence that the application of the bias voltage to switch off the electrical leakage paths (Sec. 3.1.3) also inhibits the diffusion of metallic impurities into the fused silica and the platinum, prolonging the life of SPRTs at high temperature [93]. Other options include open-sheathed SPRTs and alumina-sheathed SPRTs [95], although further research is required to confirm their suitability too. Another alternative, which may be more desirable, is to add a new subrange that includes the gold fixed point, without removing the existing subrange that terminates at the silver point.

In any of these cases, a new $W_r(T_{XX})$ function would be required to accommodate the increased temperature range. The addition of a new subrange would not be disruptive, but replacement of the silver point would be.

## 3.4 New Interpolations

Sections 2.2 and 2.5 show that the properties of the interpolating functions $F_i(W)$ are major determinants of irreproducibility of ITS-90 because they determine the interpolating errors and the propagation of uncertainties from the fixed-point realisations. That is, any significant improvements in reproducibility with ITS-XX require improved interpolating equations.

The disruption and cost of major mathematical changes will be substantial if software and firmware implementations of the new scale must be rewritten. The costs for some users might be reduced if the BIPM makes available appropriately tested and certified .dll files for computing ITS-XX temperatures. The disruption could be further reduced if the changes were only applied to subranges that extend below the argon point, since commercial devices with embedded ITS-90 mathematical functions are typically not used at temperatures below 84 K, although this may change in the future.

*3.4.1 Improved spacing of nodes*

From a mathematical perspective, the most obvious means to improve the scale reproducibility is to move the fixed points so that they are placed at the Chebyshev nodes and ensure that $|F_i(W)| \le 1.0$, and use simple polynomial interpolations for all subranges. Although the temperatures at which the fixed points occur cannot be changed, the measured resistance ratios can be shifted by applying a monotonic non-linear transformation, $Y(W)$, to all measured $W$ values so that $Y(W_i)$ fall on or close to the Chebyshev nodes. The interpolation equations in $\ln(W)$ in some of the ITS-90 interpolating equations may already have this effect. Once the $W$ values have been transformed, the interpolation can be carried out using Lagrange interpolation.

Figures 12 and 13 show this approach applied to the oxygen-water subrange. First, Figure 12 shows a simple cubic polynomial transform

$$Y(W) = A + BW + CW^2 + DW^3 \tag{47}$$

where the coefficients $A$, $B$, $C$, and $D$ are determined by requiring (47) to map the four $W_{r,i}$ values to the corresponding Chebyshev nodes (35). The transformation is then applied to all measured resistance ratios prior to a Lagrange interpolation in $Y$:

$$W_r(W) = \sum W_{r,i} F_i(Y), \tag{48}$$

where the $F_i(Y)$ are third-order Lagrange polynomials in $Y$. Figure 13, which plots the Lagrange polynomials as a function of $W$, shows that the pre-interpolation transformation ensures that $|F_i(W)| \le 1.0$ for all values of $W$ between $W_{O2}$ and 1.0. Near $W = 0.6$, the quadrature sum of the interpolating functions has been almost halved, suggesting that a substantial reduction in scale uncertainty may be possible. While the uncertainty propagation from the fixed points has certainly been improved, it remains to be seen whether the NU3 is improved.

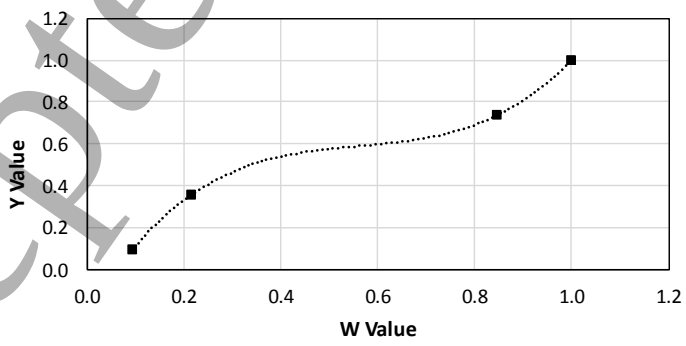


**Figure 12:** A simple cubic transformation of $W$ values ensuring that the transformed oxygen, argon, mercury and water fixed points (marked) are placed at the Chebyshev nodes of an interpolation in $Y$.

Consider also the effect of the pre-interpolation transformation on the identities $\sum F_i(W)=1$ and $\sum W_i F_i(W)=W$. The first of the identities is a property of all Lagrange interpolations, so is unchanged. However, because the inverse of (47) lies outside the vector space of the interpolation, the $\sum W_i F_i(W)=W$ identity is no longer true. If the pre-interpolation transformation is a polynomial in $Y$ (rather than $W$), *i.e.*, $W = A+BY+CY^2+DY^3$, then the polynomial lies within the vector space of the interpolating functions and

$$\begin{aligned}\sum W_i F_i(Y) &= \sum \left(A+BY_i+CY_i^2+DY_i^3\right)F_i(Y) \\ &= A+BY+CY^2+DY^3 = W.\end{aligned} \tag{49}$$

If possible, it is better to define the pre-interpolation transformations in the form $W(Y)$ rather than $Y(W)$. The applicability of both identities means that the interpolation can be expressed in terms of deviation functions, and the equations interpolate Matthiessen's rule well. To enable inverse calculations, either form of the pre-interpolation transformation must be 1:1 throughout its range.

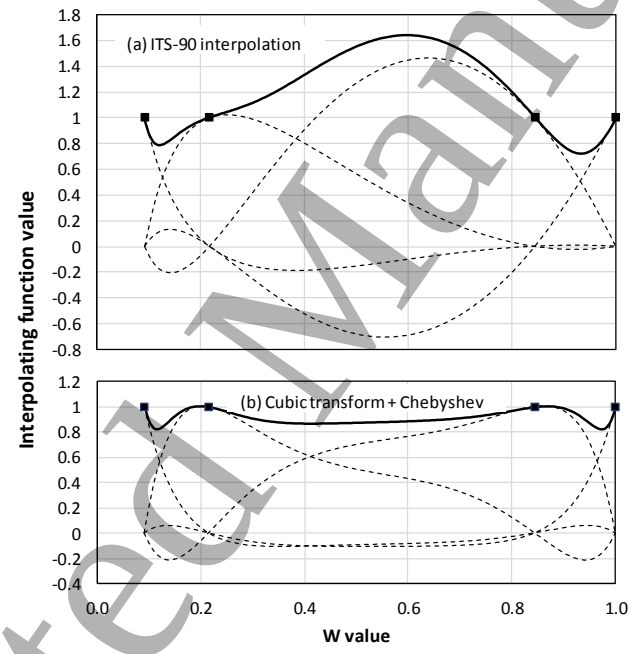


**Figure 13:** The interpolating functions $F_i(W)$ for the oxygen-water subrange using (a) the ITS-90 formulation of the interpolations, and (b) using the transformation of Figure 12 followed by a third-order Lagrange interpolation. The dashed lines are the interpolating functions, the solid lines are the quadrature sum of the functions, and the solid squares indicate the fixed points.

In addition to the much-improved uncertainty propagation and a possible improvement in NU3, improved interpolations have the possibility of making the mercury point and the two vapour pressure points unnecessary. The approach also has the advantage that every ITS-XX interpolation could be a Chebyshev interpolation. This makes it possible to use the same algorithm for all interpolations and eliminate the confusing collection of largely unrelated interpolations currently used by ITS-90.

There are some disadvantages. Firstly, every non-linear transform, whether defined as $Y(W)$ or $W(Y)$, must be different for each subrange, so that the confusing collection of ITS-90 interpolations would be replaced by an equally confusing set of pre-interpolation transformations. The main disadvantage is the rather substantial disruption to most users and instrument manufacturers.

Considerable effort, developing and investigating a variety of transformations and their effect on SRI and NU3, is required to support this approach. It may also be that no simple monotonic transform can be found for some subranges. In these cases, the use of a lower-order least-squares approximation for the transformation may offer a useful reduction in the $|F_i(W)|$ values.

One of the most interesting possibilities is that improved interpolations might be direct replacements for the ITS-90 interpolations, and therefore provide an immediate improvement in non-uniqueness without any change to the reference function.

*3.4.2 Physics-based interpolating equations*

Section 2.5 shows that the interpolation error might be reduced if the interpolating equations closely follow the actual behaviour of the SPRTs. Figure 14 shows an *S*-parameter plot for 24 capsule SPRTs measured at NRC and spanning the low-temperature subranges of ITS-90. An additional line (uppermost, with open points) plots the line $S = 1$, corresponding to the ITS-90 reference resistance ratios, which are taken from a real SPRT #217894 [96]. The plot is very different from Figure 4 for SPRTs used above the argon point in at least three important respects. Firstly, whereas Figure 4 consists of 57 lines that are approximately horizontal and mostly parallel, more than half of the lines in Figure 14 are curved and cross over other lines. That is, SPRTs follow Matthiessen's rule quite well above 80 K, but below the 80 K, their behaviour is more complicated. Secondly, in Figure 4, the *S* values for the argon points are all *lower* than the corresponding *S* values for the mercury point, whereas in Figure 14, the *S* values for the argon points are almost always *higher* than that of the mercury point. That is, there is a consistent difference in the behaviour of capsule SPRTs and long-stem SPRTs. Thirdly, the $S = 1$ line in Figure 4 passes close to the centre of the group of SPRTs, as it should to minimise SRI (Sec. 2.5). But in Figure 14 the line is at the extreme of the group. Following the discussion of Sec. 2.5, this observation suggests that the low temperature segment of the $W_r(T_{90})$ function is probably not the best choice for minimising the SRI.

Inspection of Figures 10 and 14 yields several insights into SPRT behaviour that may be useful for the development of interpolating equations. Firstly, as noted in Sec. 2.6, the collection of largely horizontal lines of the form *S* = *constant* in Figure 10 is a consequence of SPRTs closely following Matthiessen's rule. However, there is a slight divergence of the lines; lines with high *S* values tending to have a small positive slope while those with lower *S* values tend to have a small negative slope. This divergence is consistent with the observations of Berry [27], who also noted that SPRTs did not exactly follow Matthiessen's rule. As explained in Sec. 2.8, straight lines in an *S*-parameter plot indicate that SPRTs should be well described by a quadratic equation in *W*.

The fact that most SPRTs of Figure 10 follow Matthiessen's rule well means that the lines for different SPRTs do not intersect. Indeed, intersections between lines are evidence of additional physical phenomena affecting the resistance-temperature characteristic of some or all the SPRTs. An example of this occurs between the aluminium and silver points where the electrical leakage in some SPRTs causes some lines to intersect.

The large number of intersections and divergences in Figure 14 suggests several different phenomena may be affecting SPRT resistance below 80 K, and presumably the different physical effects are associated with different impurities in the platinum. Notably, there are groups of SPRTs with similar low-temperature *S* values, but their curves rapidly diverge with increasing temperature. A good example is the group of four indicated by the ellipse in the upper left of Figure 14. The differences between the diverging curves for these four SPRTs have much the same sigmoid shape. Is this a clue that might lead to more physically meaningful interpolation equations? Apart from the efforts of Nicholas to find a thermodynamic model of the resistivity of platinum [30], there have been no serious efforts to find improved models of platinum resistance in recent decades.

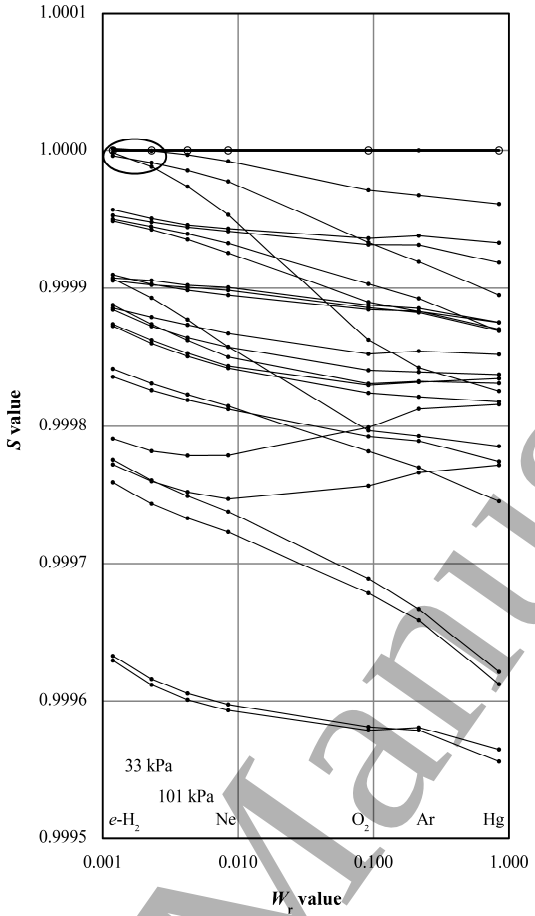


**Figure 14:** *S*-parameter plots for 24 capsule SPRTs measured at NRC spanning the low temperature subranges of ITS-90 (solid points). The additional uppermost line (with open points) corresponds to the ITS-90 reference resistance ratios. The group of four SPRTs identified by the ellipse is described in the text (Sec. 3.4.2).

## 3.5 New Subranges

The observation of Sec. 2.5, that the reproducibility of ITS-90 is determined solely by the uncertainty propagated from the fixed points and the NU3 for the subrange in use, means that new subranges can be added without damaging other aspects of the scale. Research required to support new subranges includes confirmation that the mean SRI is negligible, a determination of the NU3 for the new subranges, and may include the development of new fixed points.

*3.5.1 Linear Interpolations Below TPW*

For laboratories not requiring ITS-90 realisations at the lowest temperatures, the looming problems with the mercury fixed point can be circumvented with the use of a linear interpolation between the triple point of water and the xenon point (−111.744 °C), or sulphur hexafluoride point (−49.595 °C), or carbon dioxide point (−56.558 °C). A new subrange based on the xenon point would be especially interesting because it would span the temperature range for non-liquid-nitrogen tissue storage between −70 °C and −110 °C [89], removing the need for an argon point to reach these temperatures.

*3.5.2 High-order Interpolations Below, and Straddling, TPW*

If the new interpolation scheme described in Sec. 3.4.1 is effective in reducing the non-uniqueness of the scale, then it may be possible to construct additional low-temperature subranges, without the mercury point, to overlap the entire temperature range from 13.8 K to 273.16 K. Alternatively, new subranges could be formulated in which the mercury point is omitted and the gallium point (or an even higher-temperature fixed point) is added [46, 61]. These subranges could co-exist with the ITS-90 formulations, which would reduce the compulsion for instrument manufacturers and others to immediately adopt the changes. Indeed, the value for the resistance ratio at the mercury point could be interpolated using the new equations and fixed points, probably with a very modest increase in scale uncertainty. The use of such a 'virtual mercury point' would satisfy the needs of the many who do not require a state-of-the-art scale.

*3.5.3 Subranges Excluding the TPW*

Section 2.4, above, pointed out that the resistance ratios can be calculated relative to any fixed-point resistance. It has been suggested[1] that new subranges could be introduced that exclude the triple point of water. Examples might include linear interpolations between the gallium and indium points, or between the indium and tin points. This has the potential to increase convenience for many users by allowing cheaper and simpler ITS realizations with one less fixed point, even if it comes with a minor increase in uncertainty.

A particularly interesting possibility is a subrange between the hydrogen and argon points, which might eliminate the need for the vapour pressure points near 17 K and 20.3 K.

## 4 CONCLUSIONS

The International Temperature Scale of 1990 (ITS-90) has now been in use longer than any previous international temperature scale and the thermal metrology community has begun to consider a revision. The motivations include an opportunity to improve the thermodynamic accuracy of the scale, an opportunity to improve the reproducibility and ease of use of the scale, and an opportunity to mitigate the risk of health and safety regulations making the use of the mercury fixed points impracticable.

Section 2 collates and summarises what is known of the mathematical properties of the ITS-90 SPRT interpolations. The summary includes results drawn from previous papers, some less well-known observations drawn from CCT Working Documents, as well as several new observations. The discussion explains alternative formulations of the interpolations, the utility of the Lagrange-like formulations in uncertainty propagation and in the understanding of non-uniqueness, the origin of non-uniqueness, current best estimates of the uncertainties due to Type 1 and Type 3 non-uniqueness, and the origin of the discontinuity at the triple point of water. The most important new result is a clarification of the origin of non-uniqueness and the relationship between Type 1 (SRI) and Type 3 (NU3) non-uniqueness. The explanation resolves the debate about how best to quantify the uncertainty in the scale, as well as highlighting an opportunity to add subranges to the existing scale without incurring collateral problems. The section also highlights a lack of data supporting the assessment of uncertainty for some ITS-90 subranges.

Section 3 then considers opportunities for improvements to the scale and the research required to realise the benefits. The options range from clarifications introducible via the ITS-90 technical annex, through numerical changes preserving the algebraic structure of ITS-90, to a full overhaul of the interpolations, changes to fixed points, and addition of new subranges.

The thermodynamic accuracy of the scale can be improved substantially and easily, simply by promulgating a new reference function. Recent experiments confirm that the differences in $T-T_{90}$ are of the order of 10 mK or more, with uncertainties around 1 mK. Thus, an improvement in the scale accuracy of about a factor of ten seems achievable and would reduce the confusion between thermodynamic temperature and scale temperature as direct dissemination of thermodynamic temperature becomes more commonplace.

Improvements in the reproducibility of the scale are more difficult to realise. In principle, better chosen interpolation equations for the low temperature subranges might yield reductions in NU3 by perhaps 50% in some temperature ranges. Otherwise, other foreseeable improvements are not intrinsic to a scale revision: the claimed uncertainty in the best realisations can be reduced immediately due to the recognition that uncertainty due to

[1] Private Communications: Michael de Podesta, NPL

interpolation error is quantified simply as the Type 3 non-uniqueness (i.e., omitting the contribution due to SRI). It's possible that improvements in resistance measurements above 660 °C could reduce the uncertainty there too.

Possible solutions to the problems with the mercury point include replacement by a Xe, $SF_6$ or $CO_2$ fixed point; improved interpolating equations allowing omission of the mercury point; and new overlapping subranges. The first two of these options involve significant disruption to users of the scale. The replacement of the mercury point necessarily involves numerical changes, while improvements to the interpolating equations, so that the mercury point is no longer required, would require new equations. The third option, of promulgating additional subranges not using a mercury point, provides an alternative for many users and may simplify the scale for smaller temperature ranges. Because new subranges would be additional to the ITS-90, the changes could be incorporated into instrumentation at the manufacturers' convenience. There would be no compulsion to have changes fully implemented on the day ITS-XX is introduced.

Although the costs of a scale revision are outside the scope of this study, it is important to consider interests of all scale users when considering a revision. For most members of the thermal measurement community, a revision will probably pass unnoticed. However, for many instrumentation manufacturers and suppliers, standardising and accrediting organisations, NMIs and second-tier calibration laboratories, the costs and inconvenience may outweigh the benefits. Indeed, the benefits of improved thermodynamic accuracy and reproducibility might be appreciated by very few at present, though broader future advancements enabled by the implementation of an improved temperature scale are hard to predict. That being said, overriding the monetary concerns and inconvenience is the increasing likelihood that health and safety regulations in many countries will make the use of mercury impossible, and therefore make the realisation of low-temperature subranges of ITS-90 impossible. If we are forced to make a change, we should consider what changes can be made without causing significant disruption.

The distinguishing signature of a disruptive ITS revision is a compulsory change to any firmware or software for realising ITS-90. There are three classes of changes that have a reduced element of compulsion, and therefore likely to be less disruptive. Firstly, if a new scale is introduced that is more reproducible than ITS-90, but otherwise indistinguishable from ITS-90, then only those instrumentation manufacturers pursuing the state-of-the art need make the changes immediately, and, almost certainly, not to all instruments in their catalogues. Otherwise, manufacturers can continue to use the ITS-90, only updating instruments as required as old models are retired. In addition to the clarifications of Sec. 3.1, such changes include optimisation of the reference resistance ratios (Sec. 3.2.1) to improve the reproducibility, and possibly improved interpolations using a virtual mercury point (Sec. 3.5.2).

The second class of non-disruptive changes arise from the retention of ITS-90 but with the addition of new subranges (Sec. 3.5). This class of changes has a greater element of compulsion due to the likely competition between manufacturers to offer the benefits of the new subranges, but the timing of such changes is still optional.

The third class of non-disruptive changes comprises those modifications that affect only the subranges extending below 84 K, since much less software (mostly at NMIs) and commercial firmware accesses this range.

If an ITS revision does mandate firmware or software changes, the resulting disruption could be reduced if only numerical coefficients, rather than mathematical functional forms, need to be updated. Furthermore, some of the risks and costs of scale changes could be offset by making available proven dynamic link-library files (.dll files) with the tables of coefficients, the $W_r(T_{XX})$ function, and functions for converting between the scales.

The research required to support changes to the mathematics is largely of the form of numerical analysis, but it is critically dependent on having available a large high-quality set of measured fixed-point resistance ratios for the full set of ITS-90 fixed points and any other fixed points that might be included in a revised ITS. Comprehensive data sets of measurements between fixed points are also needed for NU3 characterisation of individual subranges. Currently, such data is only available for some of the ITS-90 SPRT subranges.

The research required to support new fixed points involves a substantial effort to evaluate the quality and availability of any new fixed-point substances, determine the reproducibility of the fixed points, and develop satisfactory fixed-point implementations for use with both capsule and long-stem SPRTs (where applicable). Once new fixed points are deemed suitable, there may be significant adoption costs related to purchasing, commissioning, and training for both the realisation technique and the associated equipment, redevelopment of technical procedures, participation in comparisons, and the costs of accreditation and regaining recognition of CMCs. It would also be necessary to consider international comparisons of the new fixed points before implementation of a new scale.

## 5 ACKNOWLEDGEMENTS

The authors gratefully acknowledge S. N. Dedyulin, M. de Podesta, K. D. Hill, G. Machin, T. Nakano, R. L. Rusby, P. Saunders, A. G. Steele, W. L. Tew, and A. D. W. Todd for helpful discussions, G. F. Strouse for long-stem SPRT data, and K. D. Hill, C. W. Meyer, A. G. Steele, and W. L. Tew for capsule SPRT data.

## 6 REFERENCES

[1] Preston-Thomas H 1990 The International Temperature Scale of 1990 (ITS-90) *Metrologia* **27**, 3-10
[2] Preston-Thomas H 1990 Erratum: The International Temperature Scale of 1990 (ITS-90) *Metrologia* **27**, 107
[3] Preston-Thomas H, Quinn T J 1992 The International Temperature Scale of 1990: Part 1, in *Temperature: Its Measurement and Control in Science and Industry*, Vol 6, Ed. J F Schooley, (American Institute of Physics, New York) pp 63-68
[4] Preston-Thomas H, Quinn T J 1992 The International Temperature Scale of 1990: Part 2, in *Temperature: Its Measurement and Control in Science and Industry*, Vol 6, Ed. J F Schooley, (American Institute of Physics, New York) pp 69-74
[5] Newell D B, Cabiati F, Fischer J, Fujii K, Karshenboim S G, Margolis H S, de Mirandes E, Mohr P J, Nez F, Pachucki K, Quinn T J, Taylor B N, Wang M, Wood B M, Zhang Z 2018 The CODATA 2017 values of *h*, *e*, *k*, and $N_A$ for the revision of the SI. *Metrologia* **55**, L13-L16
[6] Stock M, Davis R, de Mirandes E, Milton M J T 2019 The revision of the SI-the result of three decades of progress in metrology, *Metrologia* **56**, 022001
[7] Pitre L, Sparasci F, Risegari L, Guianvarc'h C, Martin C, Himbert M E, Plimmer M D, Allard A, Marty B, Giuliano Albo P A, Gao B, Moldover M R, Mehl J B 2017 New measurement of the Boltzmann constant *k* by acoustic thermometry of helium-4 gas *Metrologia* **54**, 856-873
[8] Gavioso R M, Madonna Ripa D, Steur P P M, Gaiser C, Truong D, Guianvarc'h C, Tarizzo P, Stuart F M, Dematteis R 2015 A determination of the molar gas constant *R* by acoustic thermometry in helium *Metrologia* **52**, S274-S304
[9] de Podesta M, Mark D F, Dymock R C, Underwood R, Bacquart T, Sutton G, Davidson S, Machin G 2017 Re-estimation of argon isotope ratios leading to a revised estimate of the Boltzmann constant *Metrologia* **54**, 683-692
[10] Feng X J, Zhang J T, Lin H, Gillis K A, Mehl J B, Moldover M R, Zhang K, Duan Y N 2017 Determination of the Boltzmann constant with cylindrical acoustic gas thermometry: new and previous results combined *Metrologia* **54**, 748-762
[11] Moldover M R, Gavioso R M, Mehl J B, Pitre L, de Podesta M and Zhang J T 2014 Acoustic Gas thermometry *Metrologia* **51**, R1–19
[12] Gaiser C, Zandt T, Fellmuth B 2015 Dielectric Constant Gas Thermometry *Metrologia* **52**, S217-226
[13] Gaiser C, Fellmuth B, Haft N, Kuhn A, Thiele-Krivoi B, Zandt T, Fischer J, Jusko O, Sabuga W 2017 Final determination of the Boltzmann constant by dielectric-constant gas thermometry *Metrologia* **54**, 280-289
[14] Qu J-F, Benz S P, Pollarolo A, Rogalla H, Tew W L, White D R, Zhou K 2015 Improved electronic measurement of the Boltzmann constant by Johnson noise thermometry *Metrologia* **52**, S242-256
[15] Qu J-F, Benz S P, Coakley K, Rogalla H, Tew W L, White D R, Zhou K, Zhou Z 2017 An improved electronic determination of the Boltzmann constant by Johnson noise thermometry *Metrologia* **54**, 549-558
[16] Underwood R, de Podesta M, Sutton G, Stanger L, Rusby R, Harris P, Morantz P, Machin G 2016 Estimates of the difference between thermodynamic temperature and the International Temperature Scale of 1990 in the range 118 K to 303 K *Phil. Trans. R. Soc. A* **374**, 20150048
[17] Machin G 2018 The kelvin redefined *Meas. Sci. Technol.* **29**, 022001
[18] UNEP, 2013. Minamata Convention on Mercury: Texts and annexes. UNEP Chemicals Branch, Geneva, Switzerland. Available at www.mercuryconvention.org/

[19] White D R, Saunders P 2007 Propagation of Uncertainty on Interpolated Scales *Meas. Sci. Technol.* **18**, 2157–2169

[20] BIPM 1985 *Report of the 15th Meeting of the Consultative Committee for Thermometry (1984)*, (BIPM, Paris)

[21] BIPM 1988 *Report of the 16th Meeting of the Consultative Committee for Thermometry (1987)*, (BIPM, Paris)

[22] BIPM 1991 *Report of the 17th Meeting of the Consultative Committee for Thermometry (1989)*, (BIPM, Paris)

[23] Corruccini R J 1962 Interpolation of Platinum Resistance Thermometers, 10° to 273.15 °K, in Temperature its Measurement and Control in Science and Industry Vol 3, Ed. F G Brickwedde, (Reinhold London) pp 329-338

[24] Barber C R 1962 Low-Temperature Scales 10 to 90°K in Temperature its Measurement and Control in Science and Industry Vol 3, Ed. F G Brickwedde, (Reinhold London) pp 345-350

[25] Sharevskaya D I, Stelkov P G, Borovik-Romanov A S, Astrov D N, Orlova M P 1962 On Methods of Establishment of a Practical Scale in the Range 10° to 90°K in Temperature its Measurement and Control in Science and Industry Vol 3, Ed. F G Brickwedde, (Reinhold London) pp 351-363

[26] Van Dijk H 1962 On the Use of Platinum Thermometers for Thermometry Below 90°K. A study of Two Possibilities for Relating Resistance Data for Platinum Thermometers to Each Other in Temperature its Measurement and Control in Science and Industry Vol 3, Ed. F G Brickwedde, (Reinhold London) pp 365-380

[27] Berry R J 1963 Relationship between the real and ideal resistivity of platinum *Can. J. Phys*. **41**, 946-982

[28] Berry R J 1967 Ideal resistivity of platinum below 20 °K *Can. J. Phys*. **45**, 1693-1708

[29] Corruccini R J 1965 The Sondheimer-Wilson-Kohler Formula in Platinum Resistance Thermometry, *J Res. NBS* **69C**, 283-286

[30] Nicholas J V 1995 On the thermodynamic accuracy of the ITS-90: platinum resistance thermometry below 273 K *Metrologia* **32**, 71-77

[31] Cheney E W 1982 *Introduction to Approximation Theory 2nd Ed*. (AMS Chelsea Publishing, Providence)

[32] Rivlin T J 1969 *An Introduction to the Approximation of Functions* (Waltham: Blaisdell Publishing)

[33] Trefethen L N 2013 *Approximation Theory and Approximation Practice* (Society for Industrial and Applied Mathematics, Philadelphia)

[34] White D R 2013 Some Mathematical Properties of ITS-90, In *Temperature: Its Measurement and Control in Science and Industry Vol 8*, Ed C Meyer, AIP Conf. Proc. 1552 pp81-88

[35] White D R, Ballico M, Chimenti V, Duris S, Filipe E, Ivanova A, Kartal Dogan A, Mendez-Lango E, Meyer C, Pavese F, Peruzzi A, Renaot E, Rudtsch S, Yamazawa K 2008 Uncertainties in the Realisation of the SPRT subranges of ITS-90, Working Document of the CCT, CCT/08-19rev

[36] Bloembergen P 1995 On the propagation of the uncertainty at the triple point of water, associated with the calibration of SPRTs according to the ITS-90: a case study *Metrologia* **32**, 253-257

[37] White D R, Strouse G F 2009 Observations on sub-range inconsistency in the SPRT interpolations of ITS-90 *Metrologia* **46**, 101-108

[38] Steinhart J S, Hart S R 1968 Calibration Curves for Thermistors *Deep Sea Research* **15**, 497-503

[39] Bennett A S 1972 The calibration of thermistors over the temperature range 0–30°C *Deep-Sea Res.* **19**, 157-163

[40] Chen C-C 2009 Evaluation of resistance-temperature calibration equations for NTC thermistors *Measurement* **42**, 1103-1111

[41] Mangum B W, Bloembergen P, Chattle M V, Fellmuth B, Marcarino P, Pokhodun A I 1997 On the International Temperature Scale of 1990 (ITS-90). Part I: some definitions *Metrologia* **34**, 427-429

[42] Pokhodun, A. I., Fellmuth, B., Pearce, J. V., Rusby, R. L., Steur, P. P. M., Tamura, O., Tew, W. L., White, D. R., *Guide to the Realization of the ITS-90, Chapter 5: Platinum Resistance Thermometry*, Sèvres: Bureau International de Poids et Mesures, 2016. Available at http://www.bipm.org/en/committees/cc/cct/guide-its90.html. 12 July 2016 version.

[43] Hill K D, Steele A G 2003 The Non-Uniqueness of the ITS-90: 13.8033 K to 273.16 K *AIP Conf. Proc.* **684**, 53-58

[44] Meyer C W, Tew W L, 2006 ITS-90 non-uniqueness from PRT subrange inconsistencies over the range 24.56 K to 273.16 K *Metrologia* **43**, 341-352

[45] Singh Y P, Maas H, Edler F, Zaidi Z H 1994 Correlation between the Resistance Ratios of Platinum Resistance Thermometers at the Melting Point of Gallium and the Triple Point of Mercury *Metrologia* **31**, 49-50
[46] Hill K D 1995 Inconsistency in the ITS-90 and the triple point of mercury *Metrologia* **32**, 87-94
[47] White D R 1999 Uncovering uncertainty in ITS-90: Infrequently Asked Questions, in *Proc. TEMPMEKO 99*, edited by J.F. Dubbeldam, and M. J. de Groot (Van Swinden Laboratory, Delft) pp. 35-42
[48] de Lucas J, Benyon R 1999 The Use of Correlation Between Fixed Points for the Improvement of Confidence in the Calibration of Platinum Resistance Thermometers, in *Proc. TEMPMEKO 99*, edited by J. F. Dubbeldam, M. J. de Groot (Van Swinden Laboratory, Delft) pp. 292-297
[49] Zhiru K, Jingbo L, Xiaoting L 2002 Study of the ITS-90 non-uniqueness for the standard platinum resistance thermometer in the sub-range 0 °C to 419.527 °C *Metrologia* **39**, 127–133
[50] Zhiru K, Lan J, Zhang J, Hill K D, Sun J, Chen J 2011 An Analysis of Inconsistencies Between ITS-90 Interpolations Above 0.01 °C *Int. J. Thermophys*. **32**, 68-85
[51] Sun J P, Zhang J T, Kang Z R, Duan Y 2010 Investigating the Inconsistency of ITS-90 for SPRTs in the Subrange 0 °C to 419.527 °C *Int. J. Thermophys*. **31**, 1789–1794
[52] Pearce J V, Crabb J, Elliott C J, Rusby R L 2016 Analysis of SPRT Calibration Data Obtained at NPL Since the Introduction of the ITS-90 *Int. J. Thermophys*. **37**, 124
[53] Rusby R L, Pearce J V, Elliot C J 2017 Considerations Relating to Type 1 and Type 3 Non-uniqueness in SPRT Interpolations of the ITS-90 *Int. J. Thermophys.* **38**, 186
[54] Steele A G 2005 ITS-90: Subrange inconsistency below the triple point of water *Metrologia* **42**, 289-297
[55] Steele A G, Fellmuth B, Head D I, Hermier Y, Kang K H, Steur P P M, Tew W L 2002 CCT-K2: key comparison of capsule-type standard platinum resistance thermometers from 13.8 K to 273.16 K *Metrologia* **39**, 551-571
[56] Ancsin J, Murdock E G 1990 An Intercomparison of Platinum Resistance Thermometers between 0 °C and 630 °C *Metrologia* **27**, 201-209
[57] Strouse G F 1992 NIST assessment of ITS-90 non-uniqueness for 25.5 Ω SPRTs at gallium, indium and cadmium fixed points, in *Temperature: Its Measurement and Control in Science and Industry, Vol. 6*. Ed. J.F. Schooley (AIP, New York) pp 175-178
[58] Furukawa G T, Strouse G F 2001 Investigation of the non-uniqueness of the ITS-90 in the range 660 °C to 962 °C, *Proc, TEMPMEKO 2001*, Ed. Fellmuth B., Seidel J., Scholz G., (VDE Verlag, Berlin) 553-558
[59] Ancsin J 2004 A comparison of PRTs at the Cu-Ag eutectic point (760 °C) *Metrologia* **41**, 198-203
[60] Ancsin J 2006 Non-uniqueness of ITS-90 at 548.2°C and at 156.6°C *Metrologia* **43**, 461-469
[61] Rusby R L, Stemp H, Pearce J V, Veltcheva R I 2019 Type 3 Non-uniqueness in Interpolations Using Standard Platinum Resistance Thermometers Between -196 °C and 100 °C *Int. J. Thermophys.* **40**, 103
[62] Rusby R L 2010 The Discontinuity in the First Derivative of the ITS-90 at the Triple Point of Water *Int. J. Thermophys.* **31**, 1567-1572
[63] White D R 2010 The discontinuity in $T_{90}$ at the triple point of water, Working Document of the CCT, CCT/10-35/rev1
[64] Hill K D 2015 Platinum resistivity below 273.16 K: a tale of two reference functions *Metrologia* **52**, 54-61
[65] BIPM 2017 Technical Annex for the International Temperature Scale of 1990 (ITS-90) https://www.bipm.org/utils/en/pdf/MeP_K_Technical_Annex.pdf
[66] Crovini L, Jung H J, Kemp R C, Ling S-K, Mangum B W, Sakurai H 1991 The Platinum Resistance Thermometer Range of the International Temperature Scale of 1990 *Metrologia* **28**, 317-325
[67] White D R, Arai M, Bittar A, Yamazawa K 2007 A Schottky-Diode Model of the Nonlinear Insulation Resistance Effects in SPRTs-Part 1: Theory *Int. J. Thermophys.* **28**, 1843-1854
[68] Yamazawa K, Arai M, White D R 2007 A Schottky-Diode Model of the Nonlinear Insulation Resistance in HTSPRTs-Part II: Detailed Two- and Three-Wire Measurements *Int. J. Thermophys.* **28**, 1855-1867
[69] Widiatmo J V, Harada K, Yamazawa K, Tamba J, Arai M 2015 Electrical Effect in Silver-Point Realization Due to Cell Structure and Bias Voltage Based on Resistance Measurement Using AC and DC Bridges *Int J Thermophys* **36**, 2002–2026

[70] Fischer J, de Podesta M, Hill K D, Moldover M, Pitre L, Rusby R, Steur P P M, Tamura O, White D R, Wolber L 2011 Present Estimates of the Differences Between Thermodynamic Temperatures and the ITS-90 *Int. J. Thermophys.* **32**, 12–25
[71] Underwood R, de Podesta M, Sutton G, Stanger L, Rusby R, Harris P, Morantz P, Machin G 2017 Further Estimates of ($T - T_{90}$) Close to the Triple Point of Water *Int. J. Thermophys.* **38**, 44
[72] Gavioso R M, Ripa D M, Steur P P M, Gaiser C, Zandt T, Fellmuth B, de Podesta M, Underwood R, Sutton G, Pitre L, Sparasci F, Risegari L, Gianfrani L, Castrillo A, Machin G 2016 Progress towards the determination of thermodynamic temperature with ultra-low uncertainty *Phil. Trans. R. Soc. A* **374**, 20150046
[73] Gaiser C, Fellmuth B, Haft N 2017 Primary thermometry from 2.5 K to 140 K applying dielectric-constant gas thermometry *Metrologia* **54**, 141-147
[74] Gavioso R M, Madonna Ripa D, Steur P P M, Dematteis R, Imbraguglio D 2019 Determination of the thermodynamic temperature between 236 K and 430 K from speed of sound measurements in helium *Metrologia* **56**, 045006 25 pp
[75] Rourke P M C 2019 Thermodynamic temperature of the triple point of xenon measured by refractive index gas thermometry *Metrologia* in press
[76] Hill K D 2013 An Evolutionary Approach to Updating the International Temperature Scale *AIP Conf. Proc.* **1552**, 71-80
[77] Hill K D, Steele A G 2014 The International Temperature Scale: Past, Present, and Future *NCSLI Measure J. Meas. Sci.* **9**, 60-67
[78] Pitre L, Moldover M R, Tew W L 2006 Acoustic thermometry: new results from 273 K to 77 K and progress towards 4 K *Metrologia* **43**, 142-162
[79] Bosse H, Kunzmann H, Pratt J R, Schlamminger S, Robinson I, de Podesta M, Shore P, Balsamo A, Morantz P 2017 Contributions of precision engineering to the revision of the SI *CIRP Annals-Manufacturing Technology* **66**, 827-850
[80] Hill K D, Steele A G 2005 The triple point of xenon *Metrologia* **42**, 278-288
[81] Steur P P M, Giraudi D 2014 Preliminary Measurements of the Xenon Triple Point *Int. J. Thermophys.* **35**, 604-610
[82] Rourke P M C 2016 The triple point of sulfur hexafluoride *Metrologia* **53**, L1-L6
[83] Tew W L, Quelhas K N 2018 Realizations of the Triple Point of Sulfur Hexafluoride in Transportable and Refillable Cells *J. Res. Natl. Inst. Stan.* **123**, 123013 40 pp
[84] Kawamura Y, Nakano T 2019 Evaluation of the triple point temperature of sulfur hexafluoride and the associated uncertainty at NMIJ/AIST *Metrologia* in press
[85] Steur P P M, Rourke P M C, Giraudi D 2019 Comparison of xenon triple point realizations *Metrologia* **56**, 015008 12 pp
[86] Span R, Wagner W 1996 A New Equation of State for Carbon Dioxide Covering the Fluid Region from the Triple-Point Temperature to 1100 K at Pressures up to 800 MPa *J. Phys. Chem. Ref. Data* **25**, 1509-1596
[87] Bedford R E, Bonnier G, Maas H and Pavese F 1996 Recommended values of temperature on the International Temperature Scale of 1990 for a selected set of secondary reference points *Metrologia* **33**, 133-154
[88] Dedyulin S N 2017 Sulfur Hexafluoride: A Novel Fixed Point for Contact Thermometry *Int. J. Thermophys.* **38**, 79 13 pp
[89] Shabihkhani M, Gregory M L, Wei B, Mareninov S, Lou J L, Vinters H V, Singer E J, Cloughesy T F Yonet W H 2014 The procurement, storage, and quality assurance of frozen blood and tissue biospecimens in pathology, biorepository, and biobank settings *Clin. Biochem.* **47**-5, 258-266
[90] Bedford R E, Bonnier G, Maas H, Pavese F 1990 *Techniques for Approximating the International Temperature Scale of 1990*, Sèvres: Bureau International de Poids et Mesures Available at http://www.bipm.org/utils/common/pdf/ITS-90/ITS-90-Techniques-for-Approximating.pdf.
[91] Pavese F, Molinar G 1992 *Modern Gas-Based Temperature and Pressure Measurements* (Plenum Press, New York)
[92] Bongiovanni G, Crovini L, Marcarino P 1975 Effects of dissolved oxygen and freezing techniques on the silver freezing point *Metrologia* **11**, 125-132
[93] Hill K D 2015 High-temperature platinum resistance thermometry: the problem with silver and the case for gold *Metrologia* **52**, 478-485

[94] Marcarino P, Dematteis R, Gallorini M, Rizzo E 1989 Contamination of Platinum Resistance Thermometers at High Temperature Through Their Silica Sheaths *Metrologia* **26**, 175-181
[95] Tavener J P 2015 Development of a Standard Platinum Resistance Thermometer for Use up to the Copper Point *Int J Thermophys* **36**, 2027–2035
[96] Kemp RC 1991 The Reference Function for Platinum Resistance Thermometer Interpolation between 13,8033 K and 273,16 K in the International Temperature Scale of 1990 *Metrologia* **28**, 327-332